

Dear Editor:

We are truly grateful to yours and other reviewers' comments during the open discussion of our manuscript (Evaluation of regional background particulate matter concentration based on vertical distribution characteristics. **No. acp-2015-65**). Based on these valuable comments, we have carefully addressed the referee's main concerns with this work. Please see point-by-point response to comments and the revised manuscript for details.

Thank you very much for your work concerning our paper.

Best regards

Sincerely yours

Yu-fen Zhang and Yin-chang Feng

Responses to the reviewer#1

Review of “Evaluation of regional background particulate matter concentration based on vertical distribution characteristics” by Han et al. This study presents vertical structures of meteorological parameters, turbulence, and PM in a 250 meter tower. The data presented here is valuable to study the effect of PBL on the PM diffusions. Because the region is under heavy PM pollution, this study provides some useful results. The paper analyzes seasonal variations of diffusion of PM at different levels, and some statistical methods are applied in this study. However, some definitions need to be clarified. The English in the paper needs to be improved. This paper needs to be revised before it can be accepted for publication. The detailed comments are listed as below.

Response: The definitions have been illustrated and the English in the paper has been improved. Detailed responses go as follows.

Specific comments:

Comment: P6; The definitions of the stable, neutral, and unstable conditions in Fig. 2 need to be explained.

Response: (Page 10, line 14 to Page 11, line 2, in the revised manuscript)

The gradient Richardson number (R_i) was used for classifying the atmospheric stability conditions:

$$R_i = \frac{g}{T} \left[\frac{\Delta T}{\sqrt{z_1 z_2} \ln \frac{z_2}{z_1}} + r_d \right] \times \left[\frac{\sqrt{z_1 z_2} \ln \frac{z_2}{z_1}}{\Delta u} \right]$$

where, $\Delta T = T_2 - T_1$, $\Delta u = u_2 - u_1$, T_2 and T_1 are the measured temperatures at the height of z_2 and z_1 , \bar{T} is the averaged temperature in the layer between level z_2 and z_1 , u_2 and u_1 are the measured wind speed at levels z_2 and z_1 , g is the gravitational acceleration, r_d is dry adiabatic lapse rate. According to the values of R_i , three different conditions can be distinguished: $R_i \geq 0.1$ for stable condition, $-0.1 < R_i < 0.1$ for neutral condition, and $R_i \leq -0.1$ for unstable condition.

Comment: P7; The definition of the night PBL height (NPBL) needs to be explained.

Response: (Page13, line 12 to Page 14, line 3, in the revised manuscript)

In this paper, temperature profile was observed at 15 platforms (5m, 10m, 20m, 30m, 40m, 60m, 80m, 100m, 120m, 140m, 160m, 180m, 200m, 220m and 250m) on the meteorological tower. The vertical gradient is calculated as

$$\frac{\Delta T}{\Delta Z} = \frac{T(z+1) - T(z)}{Z(z+1) - Z(z)}$$

where $T(z+1)$ and $T(z)$ represent the measured temperatures at levels $z+1$ and z , and $Z(z+1)$ and $Z(z)$ represent the altitudes at levels $z+1$ and z . The height of the nocturnal planetary boundary layer (NPBL) is determined by the bottom of positive temperature vertical gradient level, i.e. the bottom of inversion.

Comment: P8 and Fig. 5; Why the $PM_{2.5}$ concentrations are higher at noontime at 220 m than other levels? Is this due to the secondary formation?

Response: (Page 17, line 4 to line 7, in the revised manuscript)

This is mainly due to strong vertical mixing at noontime. After sunrise, the PBL starts to rapidly increase. Pollutants near the ground gradually diffuse upward. At noontime, the mixing layer is fully developed with the averaged PBL height being about 1000-1200m. Among these 4 platforms (2 m, 40 m, 120 m and 220 m), $PM_{2.5}$

concentration at 220m is the highest during noon-afternoon-time.

Comment: P2; “was 40.0 ± 20.2 , 63.6 ± 16.9 and $53.2 \pm 11.1 \mu\text{g}/\text{m}^3$, respectively, in July, August and September”. Should change to “was 40.0 ± 20.2 , 63.6 ± 16.9 and $53.2 \pm 11.1 \mu\text{g}/\text{m}^3$, in July, August and September, respectively”.

Response: The expression has been revised. **(Page 2, line 13 to line 14, in the revised manuscript)**

Comment: P2; Atmospheric particulate matter (PM) has drawn considerable attention because it has been associated with many urban environmental problems, such as acid precipitation, decreasing visibility and climate change (Zeng and Hopke, 1989; Charlson et al., 1992; Schwartz et al., 1996; Chameides et al., 1999). PM has also been implicated in human mortality and morbidity (Dockery et al., 1993; Lagudu et al., 2011). The references should include Cao et al., 2013. Tie et al., 2009. Cao J.J., X. Tie, W. Dabberdt, Z.Z. Zhao, and T. Jie, On potential acid rain enhancement in eastern China, *J. Geophys. Res.*, 118, 4834–4846, doi:10.1002/jgrd.50381, 2013.

Tie, X., D. Wu, and G. Brasseur, Lung Cancer Mortality and Exposure to Atmospheric Aerosol Particles in Guangzhou, China, *Atmos. Environ*, 43, 2375–2377, 2009.

Response: The references have been added in the introduction. **(Page 3, line 6 and line 10, in the revised manuscript)**

Comment: P3; “In addition, regional compound pollution” should be “In addition, regional air pollution” P3; “in the city cluster” should be “a cluster of cities”.

Response: The expression has been revised. **(Page 3, line 11-15, in the revised manuscript)**

Comment: P4; With the increase of vertical height, the influence of source emission on local air quality is weakening should be “With the increase of vertical height, the influence of source emission on local air quality decreases with altitude”

Response: The expression has been revised. **(Page 2, line 6, in the revised manuscript)**

Responses to the reviewer#2

Comment:

General

This is a commendable exercise in interpretation of tall tower aerosol results. In the introduction an overview over tall tower aerosol data interpretation(e.g.,Brown et al.,2013;Heintzenberg et al.,2008; Andreae et al.,2015) should put the present approach into perspective. The main weakness is a lack of quantification of the scales that are derived from the study.

Response: The overview over tall tower aerosol data interpretation(e.g.,Brown et al.,2013;Heintzenberg et al.,2008; Andreae et al.,2015) has been added in the introduction. Measurements at different heights within the boundary layer could represent different horizontal scales of pollution. According to our study, the nocturnal PM_{2.5} mass concentration time series with the 6-10 days period at the height of 220m can reflect the influence of regional pollution within 10² km away from the measurement tower. The regional scale in this study has been quantified in the revised manuscript.

Language

The English still needs substantial improvements. Examples: transform of PM_{2.5}, associated with each other among cities, vertical height, surface layer is closely related, change rules, variation rules of temperature, were in effect

Response:

The revised manuscript has been edited by a master of the English language.

Recommendation

Accept after revision according to comments

Detailed comment:

Comment: ACPD Page 14891, Line 1. What is “ regional compound pollution”

Response: (Page 3, line 11-15, in the revised manuscript)

It has been revised as “air pollution complex” (Shao et al., 2006) in the manuscript. The air pollution complex is characterized by an increase in the oxidizing capacity of the atmosphere, reduced atmospheric visibility, and the deterioration of environmental

quality throughout the entire region; It features the interactions between the sources and sinks of air pollutants, the coupling processes of the transformation of pollutants, and the synergetic environmental impacts of air pollutants (Zhu et al., 2011).

Shao M, Tang X, Zhang Y, et al. City clusters in China: air and surface water pollution[J]. *Frontiers in Ecology and the Environment*, 2006, 4(7): 353-361.

Zhu T, Shang J, Zhao D F. The roles of heterogeneous chemical processes in the formation of an air pollution complex and gray haze[J]. *Science China Chemistry*, 2011, 54(1): 145-153.

Comment: ACPD Page 14891, Line 4. “Secondary chemical reactions” have not been introduced by Chinese scientists. Refer to appropriate textbooks instead.

Response: (Page 3, line 17-18, in the revised manuscript)

In the revised manuscript, it has been modified as follows. “The origin of PM is complex. It involves both primary emissions as well as secondary particle production due to chemical reactions in the atmosphere”.

Comment: ACPD Page 14892, Line 8. Particle size distribution should be listed under “Physical method”

Response: Particle size distribution has been listed under the “physical method” in the revised manuscript. **(Page 5, line 5, in the revised manuscript)**

Comment: Page 14892, Line 22. There are established concepts in atmospheric dynamics that could be applied here more specifically such as footprints (e.g. Schmid,2002; Foken, 2008).

Response: (Page 6, line 7-14, in the revised manuscript)

To interpret the spatial representativeness of vertical measurement, the footprint concept has been added in the revised manuscript. The footprint concept is capable of linking observed data to spatial context. The integral beneath the foot-print function expresses the total surface influence on the signal measured by the sensor at height above the surface (Schmid, 2002; Ding et al., 2005; Foken, 2008). Three main factors affecting the size and shape of flux footprint are: measurement height, surface roughness, and atmospheric stability. Increase in measurement height, decrease in surface roughness, and change in atmospheric stability from unstable to stable would lead to an increase in size of the footprint and move peak contribution away from the

instrument (https://en.wikipedia.org/wiki/Flux_footprint).

Schmid H P. Footprint modeling for vegetation atmosphere exchange studies: a review and perspective [J]. *Agricultural and Forest Meteorology*, 2002, 113(1): 159-183.

Ding G, Chen Z, Gao Z, et al. The vertical structure and its dynamic characteristics of PM₁₀ and PM_{2.5} in lower atmosphere in Beijing city [J]. *Science in China, Series D*, 2005, 35(S1): 31-44.

Foken T, Nappo C J. *Micrometeorology*[M]. Springer Science & Business Media, 2008.

Comment: Page 14893, Line 24. More specific information about PM_{2.5} measurements are requested: Total time period, temporal resolution, uncertainties.

Response: (Page 7, line 21 to Page 8, line 4, in the revised manuscript)

Mass concentrations of PM_{2.5} were measured using ambient particulate monitor chemiluminescence (TEOMR-RP1400a) at four levels (2m,40m,120m, and 220m) from July 1 to September 30,2009. The monitor's data output consists of 1-hour and 24-hour average mass concentration updated every 10 minutes and on the hour ,with the precision of $\pm 1.5 \mu \text{g/m}^3$ (1-hour ave) and $\pm 0.5 \mu \text{g/m}^3$ (24-hour ave) respectively. Accuracy for mass measurement is $\pm 0.75\%$.

Comment: Page 14894, Line 3. More information is requested on the PM₁₀ sampling: PM₁₀ inlet characteristics (as function of wind speed), start/stop of the 24 h samples.

Response: (Page 8, line 6-11, in the revised manuscript)

Twenty-four hour PM₁₀ samples were collected from local Beijing time 08:00 to 07:00 the next day using medium-volume PM₁₀ samplers (TH-150,Wuhan Tianhong Intelligence Instrumentation Facility) at the heights of 10 m, 40 m, 120 m, and 220 m from August 24 to September 12, 2009. The sampler has a system of automatic constant-flow control. Flow rate of sampling in this study is 100 L min^{-1} , and the relative error of flow is less than 3%.

Comment: Page 14894, Line 20. Definition of “seasons”

Response: The four seasons were designated as March to May for spring, June-August for summer, September-November for autumn, and December-February the next year for winter. **(Page 10, line 8-11, in the revised manuscript)**

Comment: Fig 2. Typo in legend

Response: The typo error “Netural” has been corrected to “Neutral”.(**Page 13, Figure 2**)

Comment: Page 14894, Line 15. Uncertainties of chemical analyses are missing

Response: (Page 8, line 16 to Page 10, line 3, in the revised manuscript)

Filters were conditioned for 48 h in darkened desiccators before and after sampling prior to gravimetric determination. The filters were weighed on a electronic microbalance (AX205, Mettler-Toledo, LLC) with a ± 0.01 mg sensitivity in a clean room under constant temperature (20 ± 1 °C) and RH (40 ± 3 %). Samples were stored air-tight in a refrigerator at about 4 °C before chemical analyses.

Elements (Si, Ti, Al, Mn, Ca, Mg, Na, K, Cu, Zn, Pb, Cr, Ni, Co, Fe and V) were analyzed by Inductively Coupled Plasma-atomic emission spectroscopy (ICP 9000 (N+M) Thermo Electron Corporation, USA). Blank filters were processed simultaneously with sample filters. Ultrapure water, both unfiltered and filtered, and nitric acid were also analyzed. The average element values in the blanks were subtracted from those obtained for each sample filter. 10 percent of total samples were analyzed in duplicate to verify sample homogeneity. The precision and accuracy were checked by analysis of an intermediate calibration solution. Extraction efficiencies were evaluated by analysis of the certified reference material from National Research Center of CRM. The recovery value was between 85% and 110%. A calibration check was performed to ensure a relative error no more than 2% for major elements and 5% for trace elements.

Water-soluble ions (NH_4^+ , Cl^- , NO_3^- and SO_4^{2-}) were analyzed by ion chromatography (DX-120, Dionex Ltd., USA) after extraction by deionized water. External calibration was employed to quantify the ions concentrations. A calibration check with external standards was performed to ensure a relative error no more than 10%. The uncertainty contributions of the calibration curve, calibration solution, and repetitive measurement for unknown sample were taken into account. The expanded uncertainty was 3.8% with a coverage factor $k=2$.

The thermal optical carbon analyzer (Desert Research Institute (DRI) Model 2001, Atmoslytic Inc., Calabasas, CA, USA) was used to measure organic carbon (OC) and elemental carbon (EC). The heating process can be found in IMPROVE_A protocol (Chow et al., 2010, 2011; Cao et al. 2003). Field blank and lab blank were considered and all sampling concentrations were revised by blank concentration. The uncertainty

contributions of the calibration curve, calibration solution, and repetitive measurement for unknown sample were taken into account. The expanded uncertainty was 7.6% with a coverage factor $k=2$.

Chow J C, Watson J G, Chen L W A, et al. Quantification of PM_{2.5} organic carbon sampling artifacts in US networks [J]. Atmospheric Chemistry and Physics, 2010, 10(12): 5223-5239.

Chow J C, Watson J G, Robles J, et al. Quality assurance and quality control for thermal/optical analysis of aerosol samples for organic and elemental carbon [J]. Analytical and bioanalytical chemistry, 2011, 401(10): 3141-3152.

Cao J J, Lee S C, Ho K F, et al. Characteristics of carbonaceous aerosol in Pearl River Delta Region, China during 2001 winter period[J]. Atmospheric Environment, 2003, 37(11): 1451-1460.

Comment: Page 14894, Line 24. Why should a temperature profile “correlate” with height?

Response: In the revised manuscript, it has been modified as follows. The vertical profile of wind speed and temperature under different stability are shown in Fig 2. In low atmosphere, weak vertical gradient in the temperature profile was observed over 100m. Similarly, small vertical gradient in wind speed was found over 150m. **(Page 11, line 3-7, in the revised manuscript)**

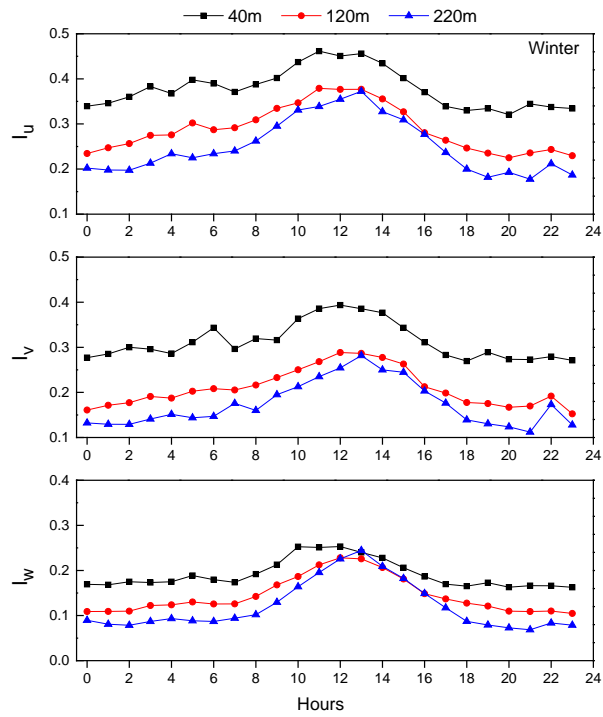
Comment: Page 14895, Line 12. Details on hourly PM₁₀ measurements are missing.

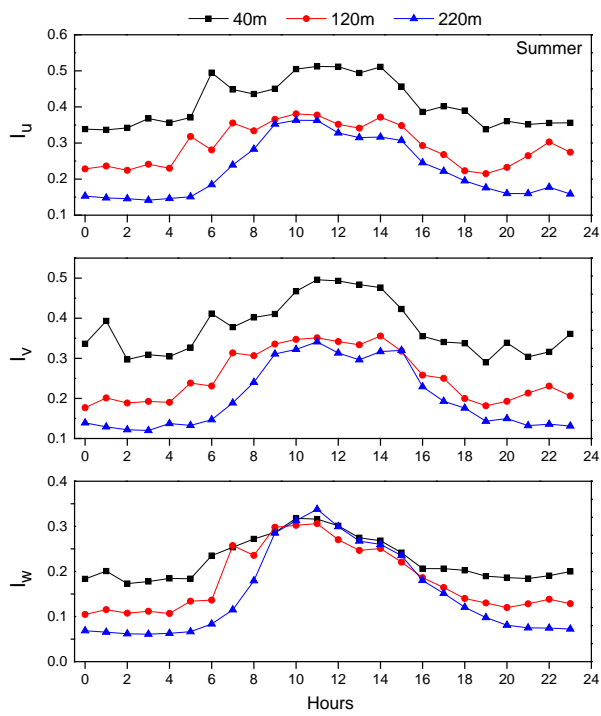
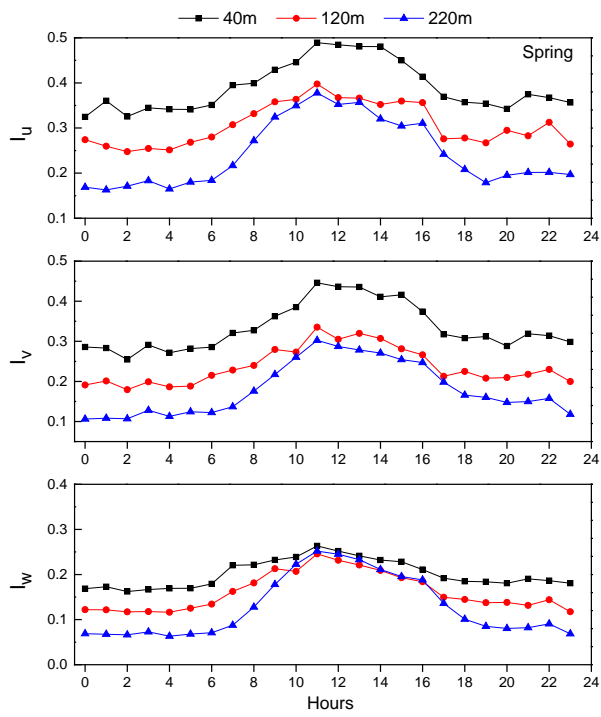
Response: The expression is not clear. It has been modified as follows. In this study, hourly averaged PM_{2.5} concentration measurement and twenty-four hour PM₁₀ sampling were conducted at four platforms (10, 40, 120, and 220m). Details on PM₁₀ sampling, as is stated above, have been added in the revised manuscript (section 2.2). **(Page 14, line 10-11; Page 8, line 6-11; in the revised manuscript)**

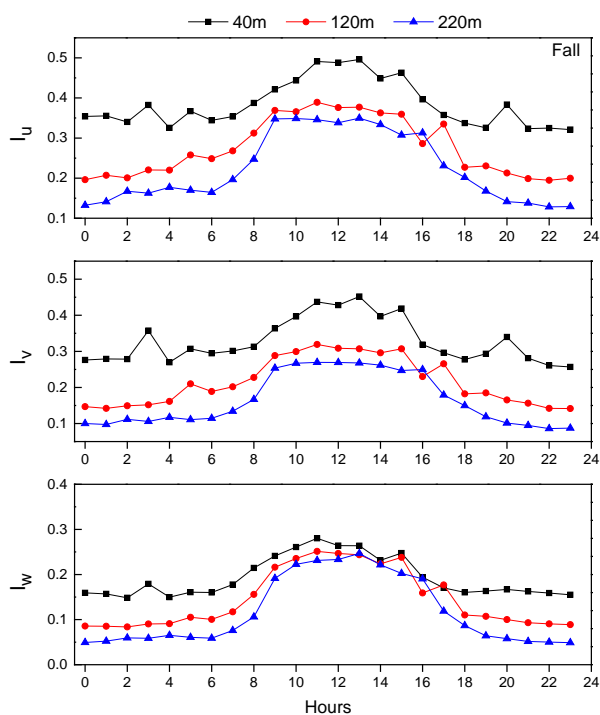
Comment: Page 14895, Line 22. Is there no seasonal variation in turbulent intensity?

Response: Diurnal variations of three dimensional components of turbulent intensity at 3 different heights in each season are shown in the Figure below (Supplemental Fig. S1 in the revised manuscript). As a whole, the averaged diurnal variations of turbulent intensity in each season were reflecting the same trends. The diurnal peaks appeared later and turbulent intensity was slightly weaker in winter than in other seasons.

(Page 15, line 5-8; Supplemental Fig. S1; in the revised manuscript;)







Supplemental Fig. S1 Diurnal variations of three dimensional components of turbulent intensity at 3 different heights in each season

Comment: Fig 5. Why are only fall data discussed and shown in Fig.5?

Response: Fig.5 shows the vertical diurnal variation of $PM_{2.5}$ mass concentrations during the period from July 1 to September 30, 2009. The four seasons were designated as March to May for spring, June-August for summer, September-November for fall, and December-February the next year for winter. Therefore part of the summer and fall data were discussed and shown in Fig.5. The title of Fig.5 has been corrected in the revised manuscript. **(Page 18, Figure 5, in the revised manuscript)**

Comment: Page 14896, Line 8. How can aerosol particles emitted near the ground “accumulate” at 120m during the night?

Response: The expression is ambiguous. In the revised manuscript, it has been modified as follows. The nocturnal planetary boundary layer (NPBL) height generally ranges from 100 m to 150 m (Fig. 3). At the 1st and 2nd platform (2m, 40 m), the measured PM are normally at inside of the NPBL. By contrast, the measurement platform at 220 m is generally outside the NPBL. The level 3 (120 m) is considered as

at the transition zone between inside and outside of the NPBL. Due to the dynamical stability of the NPBL, the vertical mixing of pollutants between inside and outside of the NPBL is very weak. The surface emitted PM are normally trapped inside the NPBL, leading to the difference in the amount of aerosols below and above the NPBL. Among these 4 platforms (2 m, 40 m, 120 m and 220 m), PM_{2.5} concentration at 220m during the night is the lowest. This indicates that the observation value of 220 m at night is less affected by local sources of emission and is largely attributed to regional scale pollution. **(Page 17, line 7-18, in the revised manuscript)**

Comment: Page 14896, Line 14. It should be possible to calculate the PBL height throughout the day and relate the vertical particle profiles to that height throughout the day.

Response: Impact of the PBL on the vertical particle profiles has been illustrated in the revised manuscript. The vertical variation patterns of PM_{2.5} concentrations were quite different during the daytime and night resulting from a combination of diurnal variations of emissions and planetary boundary layer (PBL). After sunrise, the PBL starts to rapidly increase, pollutants near the ground gradually diffuse upward and the PM_{2.5} concentration near the surface gradually decreases. At noontime, the mixing layer is fully developed with the averaged PBL height being about 1000-1200m. Among these 4 platforms (2 m, 40 m, 120 m and 220 m), PM_{2.5} concentration at 220m is the highest during noon-afternoon-time. In contrast, after 6 PM, the PBL starts to rapidly decrease. The nocturnal planetary boundary layer(NPBL) height generally ranges from 100 m to 150 m. At the 1st and 2nd platform (2 m, 40 m), the measured PM are normally at inside of the NPBL. By contrast, the measurement platform at 220 m is generally outside the NPBL. The level 3 (120 m) is considered as at the transition zone between inside and outside of the NPBL. Due to the dynamical stability of the NPBL, the vertical mixing of pollutants between inside and outside of the NPBL is very weak. The surface emitted PM are normally trapped inside the NPBL, leading to the difference in the amount of aerosols below and above the NPBL. Among these 4 platforms, PM_{2.5} concentration at 220m at night is the lowest. This indicates that the observation value of 220 m at night is less affected by local sources of emission and is largely attributed to regional scale pollution. **(Page 16, line 8 to Page 17, line 18, in the revised manuscript)**

Comment: Page 14896, Line 18. The reader still does not know where the PM₁₀ data

come from, are they the sum of all analyzed chemical components.

Response: (Page 8, line 6-11; Page 8, line 16 to Page 10, line 3; in the revised manuscript)

Twenty-four hour PM₁₀ samples were collected from local Beijing time 08:00 to 07:00 the next day using medium-volume PM₁₀ samplers (TH-150, Wuhan Tianhong Intelligence Instrumentation Facility) at the heights of 10 m, 40 m, 120 m, and 220 m from August 24 to September 12, 2009. More information on the PM₁₀ sampling and chemical analyses has been illustrated in the above responses and been added in the section 2.2 in the revised manuscript. Please see the above-mentioned response to the comments.

Comment: Page 14897, Line 5. Of what use are the coefficients of divergence?

Response: Coefficients of divergence (CD) analysis has been used to assess spatial variability. The CD values provide information on the degree of uniformity between sampling sites (Krudysz et al., 2009). In this study, CD analysis was used to assess vertical variability of chemical elements in PM₁₀ samples collected at 4 heights. **(Page 19, line 6-9, in the revised manuscript)**

Krudysz M, Moore K, Geller M, et al. Intra-community spatial variability of particulate matter size distributions in Southern California/Los Angeles[J]. Atmospheric Chemistry and Physics, 2009, 9(3): 1061-1075.

Comment: Page 14897, Line 25. Due to potentially high chlorine losses Cl as marker for sea salt is rather uncertain(Klockow et al.,1979).

Response: The chlorine loss definitely is a common phenomenon in the gas chemical processes of the sea salt. Many Cl⁻ in sea salt could be replaced by SO₄²⁻ or NO₃⁻ and released in HCl. In this study, we consider Cl⁻ as the marker of sea salt mainly because sea salt is the dominant source of Cl⁻ in our research region. Even after the potentially high chlorine losses, we still found certain amount of Cl⁻ in the PM. The purpose of the marker in this study is not to quantity how many the sea salt is, but only to get an insight into the qualitative result of the sea salt. We totally agree with the comment that such a marker may cause some uncertainty, so no definite conclusion on the sea salt's contribution was drawn in our manuscript.

Comment: Page 14898, Line 17. Are all seasons combined in the CMB modeling?

Response: Not all seasons were combined in the CMB modeling. Ambient PM₁₀ sampling in this study was conducted from August 24 to September 12, 2009. The dataset of chemical composition in the PM₁₀ samples during the measurement period were used in the CMB modeling. **(Page 22, line 9-10, in the revised manuscript)**

Comment: Fig. 7. The filtering results do not look convincing in comparison to the unfiltered data. The wild swings in the filtered data need to be justified and need to be explained in terms of underlying meteorological processes.

Response: The wild swings in the PM_{2.5} concentration data were mainly resulted from several different meteorological processes during the measurement. The data used in this study were collected at a 255-m meteorological tower which is located at the atmospheric boundary layer observation station (WMO Id.No. 54517, 39°04'29.4"N, 117°12'20.1"E) in Tianjin. According to the meteorological dataset of that station, precipitation processes were recorded during the period of 22-24 July, with the amounts of rainfall ranged from 3.2 to 94.6mm, followed by a rapid decrease in PM_{2.5} concentration on 25 July due to consequent cleaning of the air. Then, beginning on 26 July, mist paired with calm winds caused a build-up of PM_{2.5} concentration until July 29. Similar meteorological processes were reported during the period of 22-25 of August, 4-9 and 20-25 of September, which resulted in the cycle of cleaning and build-up of air pollutants. **(Page 28, line 21 to Page 29, line 5 , in the revised manuscript)**

Comment: Page 14903, Line 3. Do not report more significant figures in concentration than what corresponds to the uncertainty of the data, here certainly no more than 2 significant figures.

Response: In the revised manuscript, it has been modified as follows. The averaged regional background PM_{2.5} concentrations in July, August and September, 2009 were $40 \pm 20 \mu\text{g}/\text{m}^3$, $64 \pm 17 \mu\text{g}/\text{m}^3$ and $53 \pm 11 \mu\text{g}/\text{m}^3$, respectively. **(Page 32, line 7-8; Page 29, line 7-8; Page 2, line 13-14; in the revised manuscript)**

Comment: Page 14903, Line 13. Explain what you mean with “special stratification” in terms of standard boundary layer meteorology.

Response: The atmospheric layer at 100-150m is considered as a special stratification, the variation patterns of temperature and wind speed with height were different compared with the upper and lower layers. The vertical profile of wind speed and

temperature under different stability are shown in Fig 2. In low atmosphere, weak vertical gradient in the temperature profile was observed over 100m. Similarly, small vertical gradient in wind speed was found over 150m. Besides, from the height of 40 m to 120 m, the u, v and w components of turbulent intensity reduced by 27%, 32% and 21%, respectively. From 120 m to 220 m, the u, v and w components reduced by 12%, 13% and 15%, respectively. The descending trend is more obvious from 40 m to 120 m than that of from 120 m to 220 m. This indicates that there were fully vertical and horizontal turbulence exchanges below 120m of the tower, but relatively weaker exchanges over 120m. **(Page 30, line 12-20, in the revised manuscript)**

Comment: Page 14903, Line 20. Here and previously in the text the term regional scale needs to be quantified.

Response: Measurements at different heights within the boundary layer could represent different horizontal scales of pollution. According to our study, the nocturnal PM_{2.5} mass concentration time series with the 6-10 days period at the height of 220m can reflect the influence of regional pollution within 10² km away from the measurement tower. That is to say, regional scale is about 10² km in this study. **(Page 31, line 24-25, in the revised manuscript)**

Comment: Page 14904, Line 20. What do you mean by “better”? (also on page 14902 26)

Response: The purpose of this study is to characterize the regional pollution contribution and to evaluate regional background PM concentration levels. However, regional background concentration can hardly be measured directly. Original PM concentration time series measured on the ground reflect a combination of influence from local pollution and regional-scale pollution. A method to estimate regional background PM concentration is proposed in this paper, based on the vertical variation periodic characteristics of the atmospheric boundary layer structure and particle mass concentration, as well as the vertical distribution of chemical composition and pollution source apportionment. The measurement height influenced relatively less by local pollution emission was determined and impacts from local-scale pollution on the short-term fluctuations have been removed from the original PM concentration by wavelet transformation. After the filtering, regional-scale pollution was “better” represented in the remaining part compared with the original PM concentration time series. More explanation has been added in the

revised manuscript. (**Page 28, line 17-20; Page 30, line 2-10, in the revised manuscript**)

2 **Evaluation of regional background particulate matter concentration**
3 **based on vertical distribution characteristics**

4 S. Han^{1,2}, Y. zhang¹, J. Wu¹, X. Zhang¹, Y. Tian¹, Y. Wang¹, J. Ding¹, W. Yan¹, X. Bi¹,
5 G. Shi¹, Z. Cai², Q. Yao², H. Huang², Y. Feng¹

6 1.State Environmental Protection Key Laboratory of Urban Ambient Air Particulate Matter
7 Pollution Prevention and Control, College of Environmental Science and Engineering, Nankai
8 University, Tianjin, 300071, ChinaTianjin

9 2.Research Institute of Meteorological Science, Tianjin ,300074.

10 Correspondence to: Y.zhang (zhafox@126.com); Y. Feng (fengyc@nankai.edu.cn)

11 _____

删除的内容: Dear Editor: .
We are truly grateful to yours and other reviewers' comments during the open discussion of our manuscript (Evaluation of regional background particulate matter concentration based on vertical distribution characteristics. No. acp-2015-65). Based on these valuable comments, we have carefully addressed the referee's main concerns with this work. Please see point-by-point response to comments and the revised manuscript for details. .
.
Thank you very much for your work concerning our paper. .
Best regards .

带格式的

删除的内容: Suqin

删除的内容: Yufen

删除的内容: *

删除的内容: ianhui

删除的内容: Xiaoyong

删除的内容: Yingze

删除的内容: Yimei

删除的内容: ing

删除的内容: Wenqi

删除的内容: Xiaohui

删除的内容: Guoliang

删除的内容: Ziyang

删除的内容: Qing

删除的内容: He

删除的内容: Yinchang

删除的内容: **

带格式的: 字体: 非倾斜

带格式的: 正文, 左

删除的内容: Yufen

删除的内容: Yinchang

删除的内容: .

1 **Abstract:**

2 Heavy regional particulate matter (PM) pollution in China has resulted in an
3 important and urgent need for joint control actions among cities. It's advisable to
4 improve the understanding of regional background concentration of PM for the
5 development of efficient and effective joint control policies. With the increase of
6 ~~height~~, the influence of source emission on local air quality ~~decreases with altitude~~, but
7 the characteristics of regional pollution gradually become obvious. A method to
8 estimate regional background PM concentration is proposed in this paper, based on
9 the vertical ~~characteristics of~~ periodic ~~variation in~~ the atmospheric boundary layer
10 structure and particle mass concentration, as well as the vertical distribution of
11 particle size, chemical composition and pollution source apportionment. ~~According to~~
12 ~~the method, the averaged regional background PM_{2.5} concentration in July, August~~
13 ~~and September 2009, being extracted from the original time series in Tianjin, was 40~~
14 ~~±20µg/m³, 64 ±17 µg/m³ and 53±11 µg/m³, respectively.~~

15
16 *Key words:* particulate matter, regional background concentration, atmospheric
17 boundary layer structure, vertical ~~characteristics of~~ periodic ~~variation~~, PM chemical
18 ~~composition~~ and source apportionment

删除的内容: vertical

删除的内容: ,

删除的内容: is weakening

删除的内容: ,

删除的内容: variation

删除的内容: characteristics of

删除的内容: According to the method, the averaged regional background PM_{2.5} concentration, being extracted from the original time series in Tianjin, was 40.0 ±20.2 µg/m³, 63.6 ±16.9 µg/m³ and 53.2±11.1 µg/m³, respectively, in July, August and September.

删除的内容: variation

删除的内容: characteristics

删除的内容: component

1 Introduction

Atmospheric particulate matter (PM) has drawn considerable attention because it has been associated with many urban environmental problems, such as acid precipitation, decreasing visibility and climate change (Zeng and Hopke, 1989; Charlson et al., 1992; Schwartz et al., 1996; Chameides et al., 1999). PM has also been implicated in human mortality and morbidity (Dockery et al., 1993; Tie et al., 2009; Lagudu et al., 2011). Among the various sizes of atmospheric PM, PM_{2.5} (PM with aerodynamic diameter less than 2.5 μm) is considered to be of great significance due to its links to human respiratory health (Englert, 2004), regional-scale air pollution (Husar et al., 1981; Chameides et al., 1999), and potential acid rain enhancement (Cao et al. 2013).

The combination of rapid industrialization and urbanization has resulted in considerable environmental problems throughout China, especially in the clusters of cities (Shao et al., 2006). The coexistence of numerous air pollutants with high concentrations and the complicated interactions among them leads to the formation of an air pollution complex (Shao et al., 2006; Zhu et al., 2011). One of the major pollutants is PM (Tie et al., 2006; Liu et al., 2011; Chen et al., 2012; Han et al., 2013).

The origin of PM is complex. It involves both primary emissions as well as secondary particle production due to chemical reactions in the atmosphere (Shi et al., 2011; Tian et al., 2013; Hu et al., 2013; Guo et al., 2013). With a lifetime of days to weeks in the lower atmosphere, PM_{2.5} can be transported thousands of kilometers (Hagler et al., 2006). The trans-boundary transport of PM_{2.5} and the gaseous precursors has significant influence on the regional background PM level in the cluster of cities. In

删除的内容: .

带格式的: 缩进: 首行缩进: 0 字符

带格式的: 非突出显示

删除的内容: and

删除的内容: With

带格式的: 非突出显示

已移动(插入) [1]

删除的内容: , high PM concentration level is considered to be one of the most serious pollution problems in China (Tie et al., 2006; Liu et al., 2011; Chen et al., 2012; Han et al., 2013). In addition, regional compound pollution, such as haze and acid precipitation, has become a prominent problem.

已上移 [1]: (Tie et al., 2006; Liu et al., 2011; Chen et al., 2012; Han et al., 2013)

删除的内容: initial

删除的内容: and transform

删除的内容: may result in air pollution associated with each other among cities, which

删除的内容: y cluster

1 order to study the regional-scale PM pollution and develop efficient joint control
2 policies, it's necessary to improve understanding of regional background PM
3 concentration.

4 Background concentration has been defined as concentration observed at a site
5 "that is not affected by local sources of pollution" (WHO, 1980; Menichini et al.,
6 2007). McKendry (2006) defined background concentration as one of "those
7 pollutants arising from local natural processes together with those transported into an
8 airshed from afar (the latter may be either natural or anthropogenic in origin)".
9 Background concentration in this paper is defined to include collective contributions
10 from regional anthropogenic and natural emissions and long-range transport.

11 Background concentrations are not constant because of meteorological variability,
12 complexity of chemical reactions, as well as spatially and temporally varying
13 emissions. Regional-scale PM pollution is associated with synoptic scenarios that
14 induce the transfer, accumulation and the formation of pollutants at regional scales
15 (Ronald et al., 2007). Simply taking measurements at local scales is not well suited to
16 adequately investigate the regional background concentration. There is always the
17 possibility that the "air quality background monitoring station" is directly influenced
18 by local emission sources and thus not truly representative of the background level
19 (Tchepele et al., 2010). That is to say, background concentration can hardly be
20 measured directly, so it is critical to choose representative and appropriate values.
21 Usually, by setting some restrictions to identify and remove the influence of local
22 pollution, background concentration can be determined indirectly. There are several

1 studies mentioning the methods for determining the background concentration. These
2 methods can be classified into 4 categories. (1) The physical methods identify the
3 regional pollution process and local pollution process via synoptic situation, duration
4 of the synoptic system, consistency of vertical wind, and atmospheric stability,
5 particle size distribution, etc., and then the data of the “background period” influenced
6 by regional processes are selected (Pérez et al., 2008). (2) The chemical methods
7 identify the regional process according to chemical composition in PM and
8 synchronous observation of other pollutants, and then remove the data influenced by
9 local processes (Menichini, 2007). (3) The statistical methods use discriminant
10 analysis, cluster analysis and principal component analysis (PCA) to identify the data
11 that characterize the regional background PM (Langford et al., 2009; Tchepel et al.,
12 2010). (4) Numerical simulation methods use trajectory models and atmospheric
13 dynamics-chemical coupled models to simulate the regional background pollution
14 (Dreyer et al., 2009, Tchepel et al. 2010).

删除的内容: the

删除的内容:

删除的内容: which are

删除的内容: the size distribution or

删除的内容: of

删除的内容: the

删除的内容:

删除的内容:

15 With the increase of height, the influence of source emission on local air quality
16 decreases with altitude, but the characteristics of regional pollution gradually become
17 obvious. Influenced by atmospheric dynamics and thermal effects, meteorological
18 variables and pollutant measurements at different heights within the boundary layer
19 could represent different horizontal scales of pollution. Sites at near ground height
20 (5-10m) are influenced extensively by human activities, and the data observed at these
21 sites could represent the street scale. Impacts from local disturbance weakening with
22 height gradually and observations at greater heights could represent larger horizontal

删除的内容: vertical

删除的内容: the influence of source emission on local air quality is weakening

1 scales. When the height increases to the top of the urban atmospheric boundary layer,
2 observations can represent urban scales. Heights above the urban boundary layer
3 could to some extent reflect the characteristics of regional scales. Tall tower is
4 commonly used in observation of boundary layer meteorological,
5 micrometeorological and atmospheric chemical variables, e.g. vertical profile and
6 fluxes(Heintzenberg et al., 2008; Brown et al., 2013; Heintzenberg et al., 2013;
7 Andreae et al.,2015). The footprint concept is capable of linking observed data
8 collected at the different height levels of tower to spatial context. The integral beneath
9 the foot-print function expresses the total surface influence on the signal measured by
10 the sensor at height above the surface(Schmid, 2002; Ding et al., 2005; Foken et al.,
11 2008). Three main factors affect the size and shape of flux footprint: increase in
12 measurement height, decrease in surface roughness, and change in atmospheric
13 stability from unstable to stable would lead to an increase in size of the footprint
14 ([https://en.wikipedia.org/wiki/Flux footprint](https://en.wikipedia.org/wiki/Flux_footprint)),. Combined informations from
15 meteorological data and simultaneous aerosol measurements at the different levels of
16 the tower have allowed to gain insights into transport of aerosols and their vertical
17 distributions strongly depends on meteorological conditions, boundary layer dynamics
18 and physiochemical processes(Guinot, et al., 2006; Pal, et al., 2014). In this paper, the
19 periodic variation in the atmospheric boundary layer structure and PM mass
20 concentrations, as well as the vertical distribution characteristics of particle size,
21 chemical composition and pollution sources were studied to characterize the regional
22 pollution contribution. And on this basis, the height above which influenced relatively

带格式的：非突出显示

带格式的：字体：Times New Roman，非突出显示

带格式的：非突出显示

带格式的：字体：Times New Roman，非突出显示

带格式的：非突出显示

带格式的：字体：Times New Roman，非突出显示

带格式的：字体：Times New Roman，非突出显示

带格式的：非突出显示

删除的内容：Gradient observations of meteorological variables and ultrasonic anemometer observations can be used to analyze vertical variations of local diffusion conditions.

带格式的：非突出显示

带格式的：突出显示

带格式的：非突出显示

域代码已更改

删除的内容：The height influenced relatively less by local pollution emission can be determined and then the regional background PM concentration can be extracted from the observation data by mathematical methods

删除的内容：

删除的内容：.

删除的内容：of

删除的内容：vertical particle

1 less by local pollution emission can be determined and the regional background PM
2 concentration can be extracted from the observation data and estimate by
3 mathematical methods.

4 **2 Data sources and treatment**

5 **2.1 Observation site**

6 The data used in this study were collected at a 255 m meteorological tower which is
7 located at the atmospheric boundary layer observation station(WMO Id.No. 54517,
8 39°04'29.4"N, 117°12'20.1"E) in Tianjin, China, where is a residential and traffic
9 mixing area. There are no industrial pollution sources near the site. Tianjin is adjacent
10 to the BoHai Sea and situated in the eastern part of the Beijing-Tianjin-Hebei area,
11 one of the most heavily polluted areas in China. Tianjin covers an area of 11,300 km²
12 and has a population of 8 million. Due to rapid industrialization and urbanization in
13 recent years, air pollution has become a serious problem in this city.

14 **2.2 Observation method and data treatment**

15 Horizontal wind speed, wind direction, and temperature were measured at 15
16 platforms (5, 10, 20, 30, 40, 60, 80, 100, 120, 140, 160, 180, 200, 220, and 250 m)
17 every 10 s and averaged hourly. Three dimensional ultrasonic anemometers
18 (CAST-3D) were mounted at 40 m, 120 m and 220 m to measure the turbulent fluxes.
19 Hourly meteorological data(WMO Id.No. 54517) in the year of 2009 were used in this
20 paper.

21 Mass concentrations of PM_{2.5} were measured using ambient particulate monitor
22 chemiluminescence (TEOMR-RP1400a) at four different heights (2, 40, 120, and 220

删除的内容: to provide scientific basis for characterizing the regional pollution contribution and to evaluate regional background PM concentration levels.

删除的内容: .

删除的内容: -

带格式的: 缩进: 首行缩进: 0 字符

带格式的: 缩进: 首行缩进: 0 字符

删除的内容: m

删除的内容:

删除的内容: m

删除的内容: m

删除的内容: m

删除的内容: m

删除的内容: m

删除的内容: m

删除的内容: m

删除的内容: m

删除的内容: m

删除的内容: m

删除的内容: m

删除的内容: m

删除的内容: m

m) from July 1 to September 30, 2009. The monitor's data output consists of 1-hour and 24-hour average mass concentration updated every 10 minutes and on the hour, with the precision of $\pm 1.5\mu\text{g}/\text{m}^3$ (1-hour ave) and $\pm 0.5\mu\text{g}/\text{m}^3$ (24-hour ave) respectively. Accuracy for mass measurement is $\pm 0.75\%$.

In order to study the vertical characteristics of PM chemical composition and sources, twenty-four hour PM_{10} filter samples were collected from local Beijing time 08:00 to 07:00 the next day using medium-volume PM_{10} samplers (TH-150, Wuhan Tianhong Intelligence Instrumentation Facility) at the heights of 10 m, 40 m, 120 m, and 220 m from August 24 to September 12, 2009. The sampler has a system of automatic constant-flow control. Flow rate of sampling in this study is 100 L min^{-1} , and the relative error of flow is less than 3%. At each height, PM_{10} filter samplings were equipped with two samplers in parallel: one is for chemical analysis of inorganic composition on polypropylene filters (90 mm in diameter, Beijing Synthetic Fiber Research Institute, China) and the other is for organic composition analyses on quartz-fiber filters (90 mm in diameter, 2500QAT-UP, Pall Life Sciences).

Before and after sampling, filters were conditioned for 48 h in darkened desiccators prior to gravimetric determination. The filters were weighed on a electronic microbalance (AX205, Mettler-Toledo, LLC, with a $\pm 0.01\text{mg}$ sensitivity) in a clean room under constant temperature ($20\pm 1^\circ\text{C}$) and RH ($40\pm 3\%$). Samples were stored air-tight in a refrigerator at about 4°C before chemical analyses.

Elements (Si, Ti, Al, Mn, Ca, Mg, Na, K, Cu, Zn, Pb, Cr, Ni, Co, Fe, and V) were analyzed by Inductively Coupled Plasma-atomic emission spectroscopy (ICP

删除的内容: Hourly averaged mass concentrations of $\text{PM}_{2.5}$ were measured at four levels (2 m, 40 m, 120 m, and 220 m) by ambient particulate monitor chemiluminescence (TEOMR-RP1400a) in autumn, 2009.
带格式的: 突出显示
删除的内容: s

删除的内容: PM_{10} samples were collected at the heights of 10 m, 40 m, 120 m, and 220 m from August 24 to September 12, 2009.
删除的内容: samples
删除的内容: collected
删除的内容: using

带格式的: 字体: 非加粗
带格式的: 字体: (默认) 宋体
带格式的: 字体: (默认) 宋体
带格式的: 字体: (中文) 方正姚体

1 9000(N+M)Thermo Electron Corporation, USA). Blank filters were processed
2 simultaneously with sample filters. Ultrapure water, both unfiltered and filtered, and
3 nitric acid were also analyzed. The average element values in the blanks were
4 subtracted from those obtained for each sample filter. 10 percent of total samples were
5 analyzed in duplicate to verify sample homogeneity. The precision and accuracy were
6 checked by analysis of an intermediate calibration solution. Extraction efficiencies
7 were evaluated by analysis of the certified reference material from National Research
8 Center of CRM. The recovery value was between 85% and 110%. Calibration check
9 was performed to ensure a relative error no more than 2% for major elements and 5%
10 for trace elements.

11 Water-soluble ions(NH_4^+ , Cl^- , NO_3^- , and SO_4^{2-}) were analyzed by ion
12 chromatography (DX-120, Dionex Ltd., USA) after extraction by deionized water.
13 External calibration was employed to quantify the ions concentrations. A calibration
14 check with external standards was performed to ensure a relative error no more than
15 10%. The uncertainty contributions of the calibration curve, calibration solution, and
16 repetitive measurement for unknown sample were taken into account. The expanded
17 uncertainty was 3.8% with a coverage factor $k=2$.

18 The thermal optical carbon analyzer (Desert Research Institute (DRI) Model 2001,
19 Atmoslytic Inc., Calabasas, CA, USA) was used to measure organic carbon (OC) and
20 elemental carbon (EC). The heating process can be found in IMPROVE A protocol
21 (Chow et al., 2010, 2011; Cao et al., 2003). Field blank and lab blank were considered
22 and all sampling concentrations were revised by blank concentration. The uncertainty

contributions of the calibration curve, calibration solution, and repetitive measurement for unknown sample were taken into account. The expanded uncertainty was 7.6% with a coverage factor $k=2$.

3 Vertical variation characteristics of urban boundary structure

3.1 Thermal and dynamic characteristics in surface layer

Surface layer has a remarkable effect on the diffusion of air pollutants. This layer is strongly affected by the human behavior on the ground. Figure 1 presents on diurnal variation of averaged wind speed in four seasons at different heights in Tianjin. The four seasons were designated as March to May for spring, June-August for summer, September-November for autumn, and December-February the next year for winter. Diurnal variation patterns of wind speed were similar in each season. The wind speed is high in daytime and low at night below 100m, whereas low wind speed in daytime and high at night above 100m.

Figure 2 shows the vertical profile of wind speed and temperature in low atmosphere under different stability. The gradient Richardson number (R_i) was used for classifying the atmospheric stability conditions:

$$R_i = \frac{g}{T} \left[\frac{\Delta T}{\sqrt{z_1 z_2} \ln \frac{z_2}{z_1}} + r_d \right] \times \left[\frac{\sqrt{z_1 z_2} \ln \frac{z_2}{z_1}}{\Delta u} \right] \quad (1)$$

Where, $\Delta T = T_2 - T_1$, $\Delta u = u_2 - u_1$, T_2 and T_1 are the measured temperatures at the height of z_2 and z_1 , \bar{T} is the averaged temperature in the layer between level z_2 and z_1 , u_2 and u_1 are the measured wind speed at levels z_2 and z_1 , g is the gravitational acceleration, r_d is dry adiabatic lapse rate. According to the values of

删除的内容: All samples were collected in a 24-hr period every day and at a flow rate of 100 L/min.

删除的内容: Elements (Si, Ti, Al, Mn, Ca, Mg, Na, K, Cu, Zn, As, Pb, Cr, Ni, Co, Cd, Hg, Fe and V) were analyzed by Inductively Coupled Plasma-atomic emission spectroscopy (ICP 9000(N+M)Thermo Electron Corporation, USA). Water-soluble ions (Na^+ , K^+ , Ca^{2+} , Mg^{2+} , NH_4^+ , NO_3^- and SO_4^{2-}) were analyzed by ion chromatography (DX-120, Dionex Ltd.

带格式的: 突出显示

删除的内容: near

删除的内容: i

删除的内容: s closely related to

删除的内容: ure

删除的内容:

删除的内容: shows

删除的内容: Similar change rules

删除的内容: while,

带格式的

域代码已更改

删除的内容: .

域代码已更改

带格式的

域代码已更改

域代码已更改

带格式的

带格式的

域代码已更改

域代码已更改

域代码已更改

域代码已更改

域代码已更改

域代码已更改

域代码已更改

域代码已更改

域代码已更改

域代码已更改

1 R_i , three different conditions can be distinguished: $R_i \geq 0.1$ for stable condition,

2 $-0.1 < R_i < 0.1$ for neutral condition, and $R_i \leq -0.1$ for unstable condition.

3 The atmospheric layer at 100-150m is considered as a transition layer, the variation
4 patterns of temperature and wind speed with height were different compared with the
5 upper and lower layers. Weak vertical gradient in the temperature profile was
6 observed over 100m. Similarly, small vertical gradient in wind speed was found over
7 150m.

域代码已更改

域代码已更改

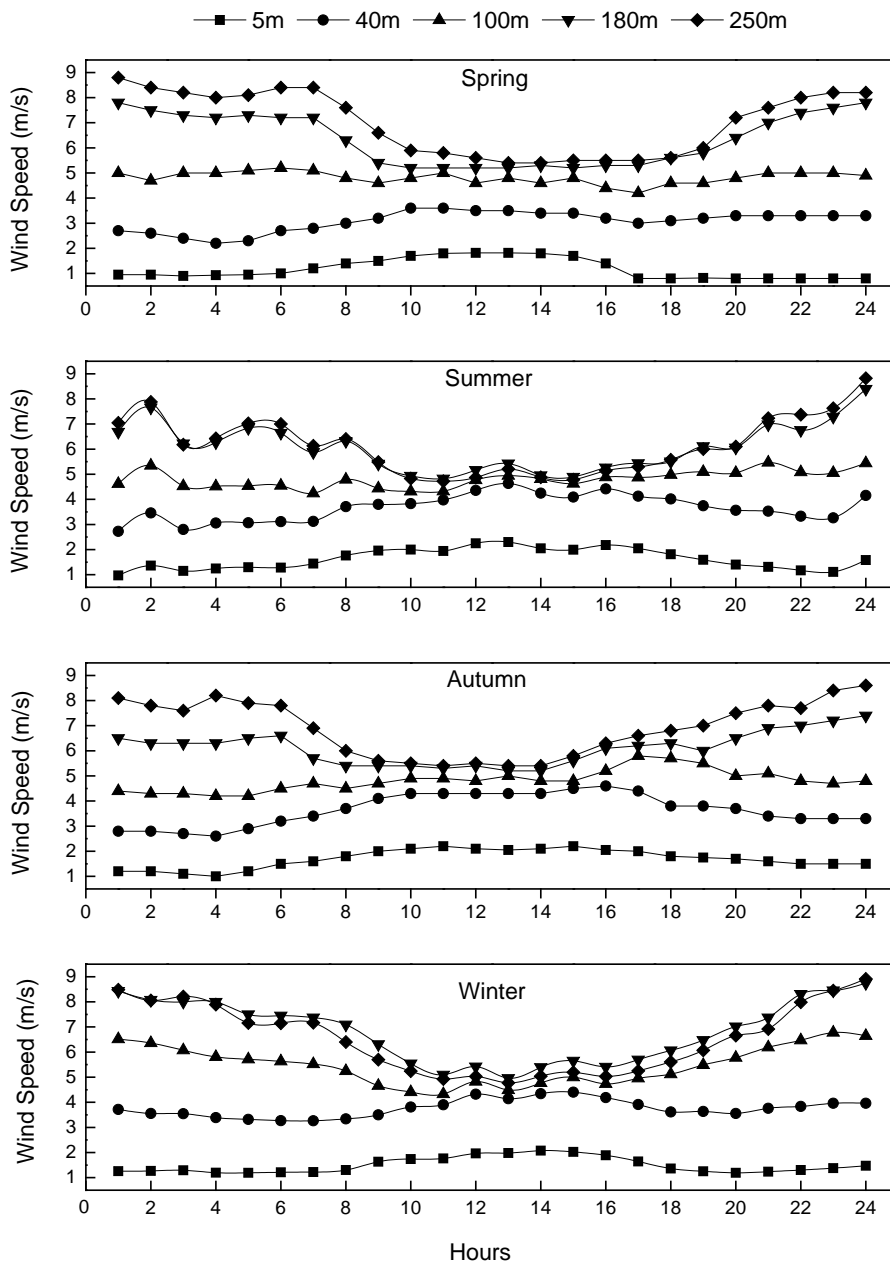
域代码已更改

域代码已更改

删除的内容: The vertical distribution profile of wind speed and temperature under different stability are shown in Figure 2. The temperature profile correlates weakly with height over 100m and the wind speed profile correlates weakly with height over 150m.

带格式的: 突出显示

删除的内容: The atmospheric layer at 100-160m is considered as a special stratification, the variation rules of temperature and wind speed with height were different compared with the upper and lower layers.



1

2 Figure 1. Diurnal variation of averaged wind speed in each season at different heights

3

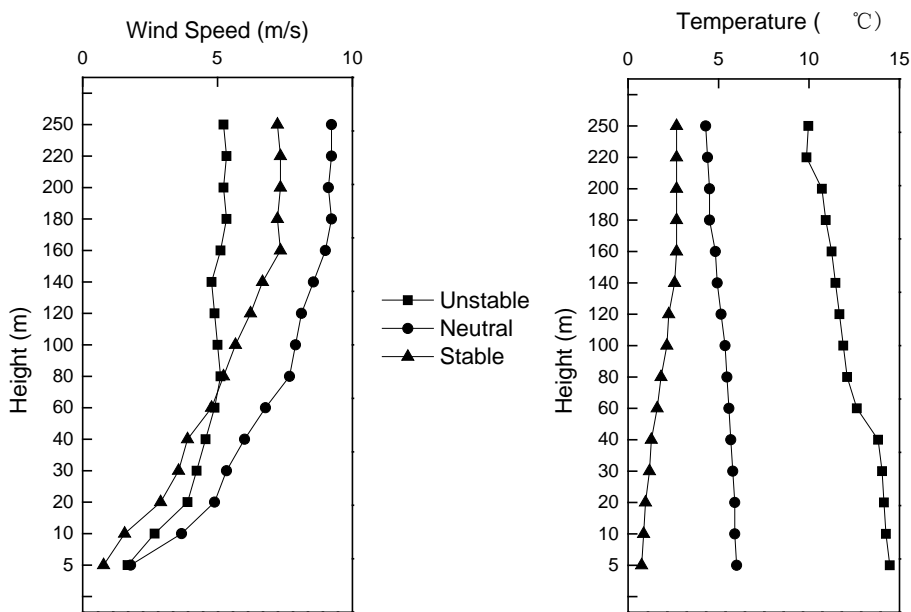


Figure 2. Vertical distribution profile of average wind speed and temperature in low atmosphere under different stability

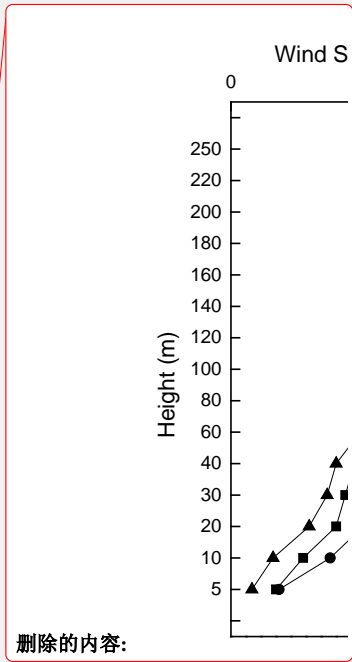
3.2 The height of nocturnal planetary boundary and vertical variation of turbulent intensity

The height of the planetary boundary layer (PBL), indicating the range of pollutants diffused by thermal turbulence in the vertical direction (Kim et al., 2007; Lena and Desiato, 1999), can be calculated by wind and temperature profiles (Seibert et al.,

2000; Han et al., 2009). Based on the temperature profile observed at the tower, the vertical gradient of temperature was calculated as:

$$\frac{\Delta T}{\Delta Z} = \frac{T(z+1) - T(z)}{Z(z+1) - Z(z)}$$

where $T(z+1)$ and $T(z)$ represent the measured temperatures at levels $z+1$ and



删除的内容:
域代码已更改

删除的内容: 2009

删除的内容:

带格式的: 首行缩进: 0 字符

域代码已更改

带格式的: 字体: 小四

带格式的: 缩进: 首行缩进: 0 字符

域代码已更改

域代码已更改

域代码已更改

z , $Z(z+1)$ and $Z(z)$ represent the altitudes at levels $z+1$ and z . The height of the nocturnal planetary boundary layer (NPBL) is determined by the bottom of the inversion, i.e. the layer in which temperature profile presents positive gradient. As shown in Figure 3, the seasonal variation of the NPBL height is generally small, with seasonal averaged NPBL height ranging from 114 to 142 m.

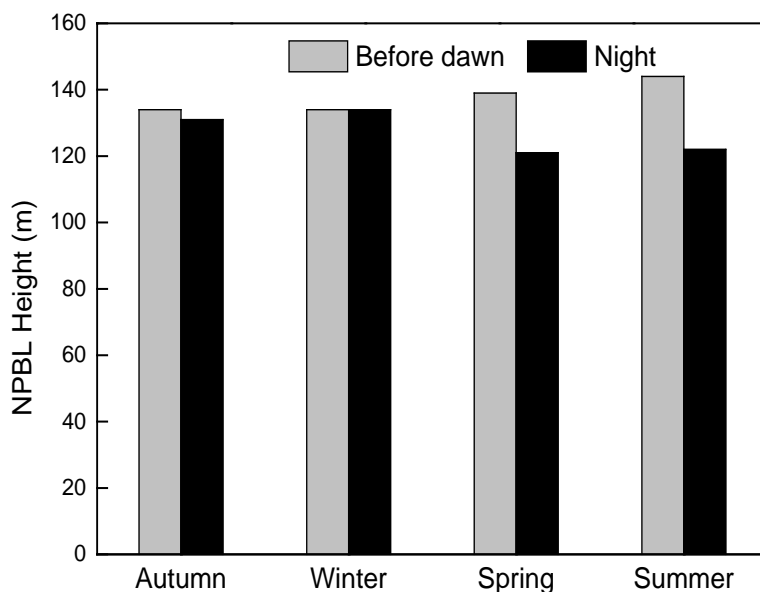


Figure 3. Averaged NPBL height in each season (before dawn 1:00-7:00; at night:19:00-24:00)

In this study, hourly averaged $PM_{2.5}$ concentration measurement and twenty-four hour PM_{10} filter sampling were conducted at four platforms. The heights of the 1st and 2nd platform are inside the NPBL, the 3rd platform is located at the top of the NPBL and the 4th platform is generally outside the NPBL. Due to the dynamical stability of the NPBL, air pollutants in surface layer are normally trapped inside the

域代码已更改
域代码已更改
域代码已更改
域代码已更改
域代码已更改

带格式的：缩进：首行缩进： 0 字符

删除的内容：
$$\frac{\Delta T}{\Delta Z} = \frac{T(z+1) - T(z)}{Z(z+1) - Z(z)}$$

In this paper, temperature gradient data observed at the tower were used to analyze the nocturnal planetary boundary layer height (NPBL) in different seasons (Figure 3). The seasonal variation of the NPBL height is generally small, with seasonal averaged NPBL height ranging from 114 m to 142 m

删除的内容： .

删除的内容： In this paper, hourly averaged mass concentrations of $PM_{2.5}$ and PM_{10} were measured at four platforms (2m, 40m, 120m, and 220m)

带格式的：非上标/ 下标

带格式的：非上标/ 下标

带格式的：非上标/ 下标

删除的内容：

带格式的：非上标/ 下标

1 NPBL and rarely mix with the pollutants outside the NPBL. Very different
2 distribution characterizations of PM were measured inside and outside the NPBL (See
3 section 4).

4 Based on the observation data from the three dimensional ultrasonic anemometers,
5 the turbulent intensity were calculated. As a whole, the averaged diurnal variations of
6 turbulent intensity in each season(Supplemental Fig. S1) were reflecting the same
7 trends. The diurnal peaks appeared later and turbulent intensity was slightly weaker in
8 winter than in other seasons. Averaged diurnal variation of turbulent intensity at
9 different heights during the year of 2009 is shown in Fig. 4. Three dimensional
10 components of turbulent intensity decreased with increase in height. From the height
11 of 40m to 120 m, the u, v and w components of turbulent intensity reduced by 27%,
12 32% and 21%, respectively. From 120 to 220 m, the u, v and w components reduced
13 by 12%, 13% and 15%, respectively. The descending trend is more obvious from 40
14 to 120 m than that of from 120 to 220 m. This indicates that there were fully vertical
15 and horizontal turbulence exchanges below 120m of the tower, but relatively weaker
16 exchanges over 120m.

带格式的：非突出显示

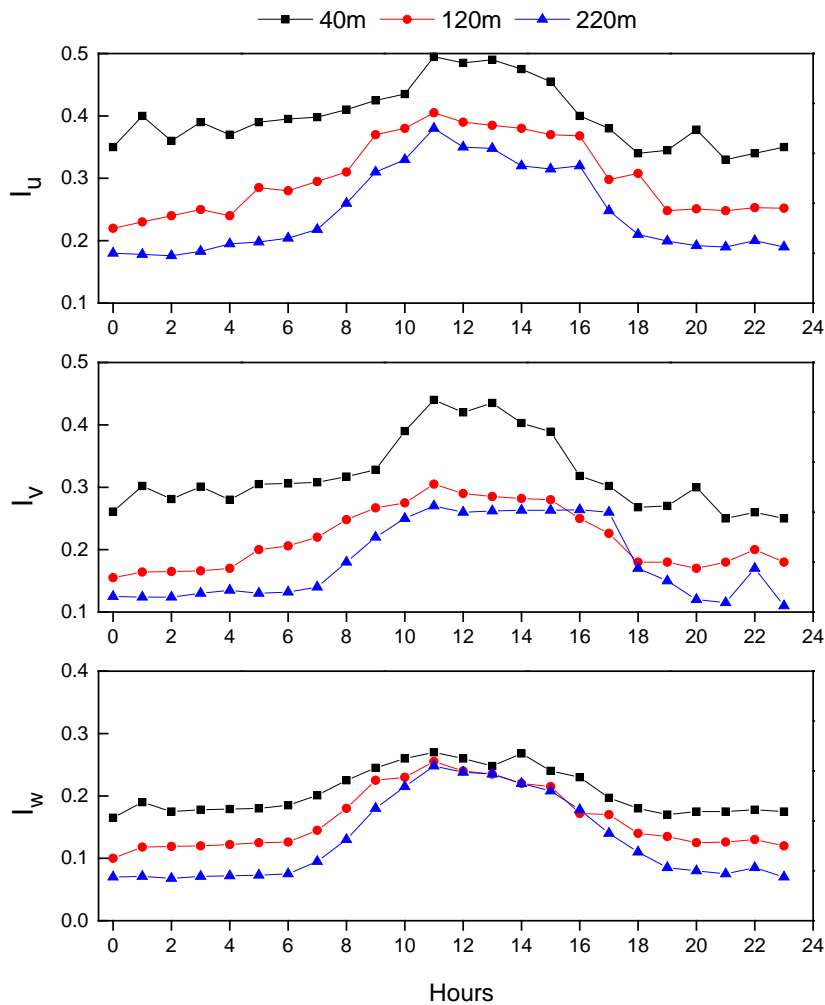
删除的内容：A

删除的内容：ure

删除的内容：m

删除的内容：m

删除的内容：m



1
2 Figure 4. Averaged diurnal variation of three dimensional components of turbulent intensity at
3 different heights (longitudinal turbulent intensity I_u , lateral turbulent intensity I_v , vertical
4 intensity I_w)

6 4 Vertical distribution of $PM_{2.5}$ mass concentration

7 The diurnal variation of $PM_{2.5}$ mass concentrations during the period from July 1 to
8 September 30, 2009 is shown in Fig. 5. The vertical variation patterns of $PM_{2.5}$
9 concentrations were quite different during the daytime and night resulting from a

删除的内容: vertical

删除的内容: Figure

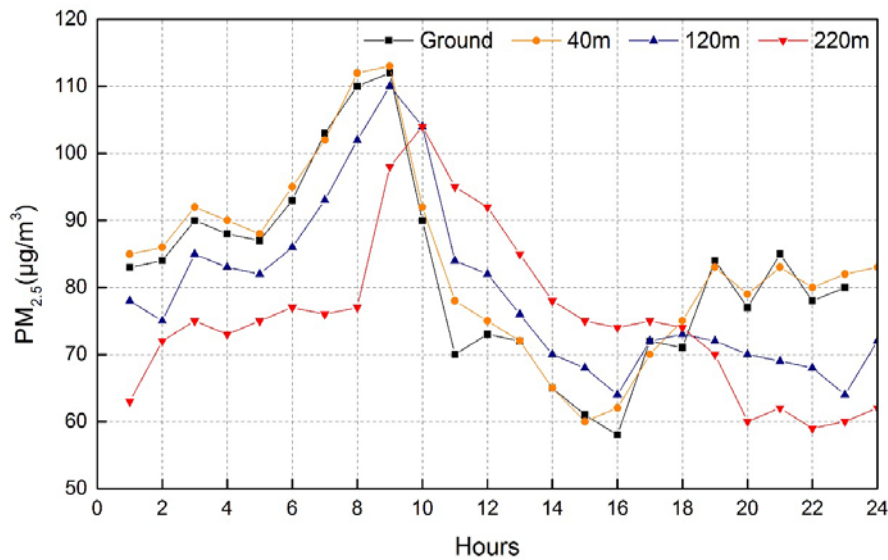
删除的内容: Among these 4 platforms (2 m, 40 m, 120 m and 220 m), $PM_{2.5}$ concentration at 220m at night is the lowest. The NPBL height generally ranges from 100 m to 150 m in Tianjin, and the height of 220 m is just outside the NPBL. This indicates that the observation value of 220 m at night is less affected by local sources of emission and is largely attributed to regional scale pollution.

1 combination of diurnal variations of emissions and planetary boundary layer (PBL).
2 After sunrise, the PBL height starts to rapidly increase, pollutants near the ground
3 gradually diffuse upward and the PM_{2.5} concentration near the surface gradually
4 decreases. At noontime, the mixing layer is fully developed with the averaged PBL
5 height being about 1000-1200m. Among these 4 platforms (2 m, 40 m, 120 m and 220
6 m), PM_{2.5} concentration at 220m is the highest during noon-afternoon-time. In
7 contrast, after 6 PM, the PBL height starts to rapidly decrease. The nocturnal
8 planetary boundary layer(NPBL) height generally ranges from 100 m to 150 m(Fig.
9 3). At the 1st and 2nd platform (2, 40 m), the measured PM are normally at inside of
10 the NPBL. By contrast, the measurement platform at 220 m is generally outside the
11 NPBL. The level 3 (120 m) is considered as at the transition zone between inside and
12 outside of the NPBL. Due to the dynamical stability of the NPBL, the vertical mixing
13 of pollutants between inside and outside of the NPBL is very weak. The surface
14 emitted PM are normally trapped inside the NPBL, leading to the difference in the
15 amount of aerosols below and above the NPBL. Among these 4 platforms, PM_{2.5}
16 concentration at 220m during the night is the lowest. This indicates that the
17 observation value of 220 m at night is less affected by local sources of emission and is
18 largely attributed to regional scale pollution.

带格式的：非上标/ 下标

带格式的：非上标/ 下标

删除的内容: At night, the pollutants emitted from the surface diffuse upwards and accumulate in the NPBL. This leads to the highest concentration of PM_{2.5} at the height of 120 m, which is near the top of the NPBL. After sunrise, the inversion layer is gradually destroyed, pollutants near the ground gradually diffuse upward and the PM_{2.5} concentration near the surface gradually decreases. At the height of 120m and 220m, the peak of pollutant concentration appears at approximately 8:00 and 9:00 respectively. At noontime, the mixing layer is fully developed and three observation levels are all inside the PBL.



带格式的：居中，缩进：首行缩进：1 字符，定义网格后自动调整右缩进，段落间距段前：0 磅，段后：0 磅

Figure 5. Vertical diurnal variation of PM_{2.5} mass concentrations during the period from July 1 to September 30, 2009

删除的内容: Vertical diurnal variation of PM_{2.5} mass concentration in Fall .

5 Vertical distributions of PM₁₀ concentration, composition and source apportionment

带格式的：字体：五号

带格式的：字体：五号，下标

带格式的：字体：五号

删除的内容: components

5.1 Vertical characteristics of PM₁₀ concentration

As mentioned in section 2.2, PM₁₀ filter samples were collected at the heights of 10, 40, 120 and 220 m. The daily concentrations at each sampling height were $139 \pm 45 \mu\text{g}/\text{m}^3$, $121 \pm 43 \mu\text{g}/\text{m}^3$, $110 \pm 39 \mu\text{g}/\text{m}^3$ and $79 \pm 37 \mu\text{g}/\text{m}^3$, respectively. These concentrations exhibited a general decreasing trend with the increase of height.

删除的内容: m

删除的内容: m

删除的内容: m

The height-to-height correlation coefficients of the variation of PM₁₀ concentration were calculated and listed in Table 1. All the pairwise correlation coefficients among 10, 40 and 120 m were higher than 0.9. However, the correlation coefficients between 220 m and other heights were obviously low. These results suggest that the influences

删除的内容: m

删除的内容: m

1 of local emissions and local meteorological diffusion conditions on PM₁₀
 2 concentrations are weaker at 220 m than that at lower levels.

3 Table1 Height-to-height correlation coefficient of PM₁₀ concentration

	10 m	40 m	120 m	220 m
10 m	1.0	.		
40 m	0.96	1.0		
120 m	0.91	0.94	1.0	
220 m	0.72	0.76	0.85	1.0

4
 5 **5.2 Vertical characteristics of PM₁₀ chemical composition**

6 Coefficients of divergence (CD) analysis (Wongphatarakul et al., 1998; Krudysz et
 7 al., 2009) was used in this study to assess vertical variability of chemical elements in
 8 PM₁₀ filter samples collected at 4 heights. The CD values provide information on the
 9 degree of uniformity between sampling sites and is defined as,

10
$$CD_{jk} = \sqrt{\frac{1}{p} \sum_{i=1}^p \frac{x_{ij} - x_{ik}}{x_{ij} + x_{ik}}^2}$$
 (3)

11 where, x_{ij} is the average concentration of the i th element at j th height. j and k
 12 represent the two sampling heights, and p is the number of elements. When the
 13 species concentrations at two sampling sites were similar to each other, the CD values
 14 would approach 0. On the other hand, as the two species concentrations diverge the
 15 CD value will approach 1 (Hwang et al., 2008).

16 The pair-wise CD values for four heights are shown in Table 2. The pair-wise CD
 17 values among 10, 40, and 120m are lower than 0.2, illustrating that the element
 18 profiles of these three heights were similar to each other. While, the CD values
 19 between 220m and the other three levels were obviously high. This may be resulted

删除的内容: components

删除的内容: Nineteen elements were analyzed from PM₁₀ samples collected at four heights.

带格式的: 非突出显示

删除的内容: In order to study the vertical variations of element profiles at the four heights, coefficients of divergence (CD) (Wongphatarakul et al., 1998; Hwang et al., 2008) were used. CD can be calculated as following:

删除的内容:
$$CD_{jk} = \sqrt{\frac{1}{p} \sum_{i=1}^p \left(\frac{x_{ij} - x_{ik}}{x_{ij} + x_{ik}} \right)^2}$$

域代码已更改

删除的内容:

删除的内容: 4

删除的内容: x_{ij}

删除的内容: i th

带格式的: 字体: (默认) Arial Unicode MS, (中文) Arial Unicode MS, 小四

带格式的: 字体: (默认) Arial Unicode MS, (中文) Arial Unicode MS, 小四

带格式的: 字体: (默认) Arial Unicode MS, (中文) Arial Unicode MS, 小四

域代码已更改

域代码已更改

删除的内容: i th

带格式的

带格式的

域代码已更改

域代码已更改

删除的内容: p

删除的内容: m

删除的内容: m

删除的内容: , indicating a larger ...

1 from that chemical elements in the PM₁₀ filter samples collected at 220m were mainly
2 originated from regional-scale sources.

删除的内容: the

删除的内容: of

3 Table 2 Pair-wise CD values at different heights

	10 m	40 m	120 m
40 m	0.10		
120 m	0.15	0.11	
220 m	0.33	0.30	0.59

4
5 The concentration of chemical composition in ambient PM₁₀ filter samples
6 collected at 4 heights are shown in Table 3. Al, Si, Ca, OC, EC, Cl⁻, NO₃⁻ and SO₄²⁻
7 have higher concentration levels than other species. Al can be used as a source marker
8 of coal combustion (Hopke, 1985) ; Al and Si are the markers of soil dust (Liu et al.,
9 2003), Ca is mainly emitted from cement dust (Shi et al., 2009) ; EC can be identified
10 as vehicle exhaust emission (Li et al., 2004) ; Cl⁻ is the marker for sea salt (Li et al.,
11 2004); and NO₃⁻ and SO₄²⁻ are the markers of secondary nitrate and sulfate (Liu et al.,
12 2003). Higher concentrations were found at lower sampling heights for almost all

删除的内容: components

删除的内容: of

删除的内容: sites

13 species (NO₃⁻ had the highest value at 120 m). Unlike the species concentration, the
14 vertical distribution of species percentages (%) shows different patterns. Similar
15 fraction levels were observed at the four heights for Al and Si. For Ca and EC, higher
16 values were observed at lower sampling sites. The percentages of OC at 220 m were
17 obviously higher than those at 120 m. This might imply that the influence of local
18 sources on OC was weaker and the contributions from secondary and regional sources
19 were larger at 220 m. The OC/EC ratios increased gradually from 10 m to 220 m. This
20 might be due to a relatively higher percentage of SOC in OC at higher heights as

1 results of the formation and regional transport of SOC (Strader et al., 1999). Similarly,
 2 the higher sampling sites obtained higher fractions (%) for NO₃⁻ and SO₄²⁻ (the highest
 3 percentage of NO₃⁻ were observed at 120m). These trends suggest that the impact of
 4 primary sources from the ground decreased with the increase of height, while the
 5 impact of secondary sources mainly influenced by regional sources becomes more
 6 prominent.

7 | Table 3 The concentration of chemical composition in ambient PM₁₀ at 4 height sampling sites (μg
 8 m⁻³)

	10m		40m		120m		220m	
	mean	sd ^a	mean	sd	mean	sd	mean	sd
Na	1.60	0.71	1.34	0.58	1.28	0.48	0.89	0.41
Mg	1.51	0.54	1.29	0.92	0.99	0.52	0.54	0.36
Al	6.3	2.5	5.9	2.1	4.9	1.7	4.0	1.7
Si	8.5	4.6	6.8	2.9	6.4	2.8	4.9	2.8
P	ND	ND	ND	ND	ND	ND	ND	ND
K	1.41	0.72	1.02	0.44	1.11	0.68	0.70	0.35
Ca	7.1	2.8	5.1	2.0	4.6	2.2	2.5	1.6
Ti	0.23	0.12	0.19	0.12	0.24	0.20	0.29	0.53
V	ND	ND	ND	ND	ND	ND	ND	ND
Cr	0.04	0.03	0.04	0.03	0.05	0.04	0.04	0.04
Mn	0.09	0.05	0.06	0.03	0.06	0.03	0.04	0.02
Fe	2.51	1.22	2.08	1.21	1.92	1.09	1.09	0.80
Ni	0.01	0.02	0.01	0.01	0.02	0.03	0.03	0.05
Co	0.01	ND	ND	ND	ND	ND	0.01	0.01
Cu	0.20	0.17	0.14	0.22	0.09	0.13	0.02	0.03
Zn	0.69	0.32	0.60	0.31	0.55	0.28	0.27	0.16
Br	ND	ND	ND	ND	ND	ND	ND	ND
Ba	ND	ND	ND	ND	ND	ND	ND	ND
Pb	0.06	0.06	0.06	0.06	0.05	0.05	0.03	0.03
OC ^a	13.5	6.2	10.8	4.6	9.6	3.8	7.3	3.1
EC ^a	7.0	2.2	5.3	2.0	4.4	1.8	3.0	1.6
NH ₄ ⁺	6.2	3.5	6.3	3.4	6.9	3.1	5.7	4.0
Cl ⁻	6.4	5.3	5.6	4.1	5.0	3.0	1.7	1.2
NO ₃ ⁻	18.0	12.5	16.9	10.9	18.9	10.1	13.3	11.4
SO ₄ ²⁻	27.4	20.6	26.1	17.5	25.3	16.4	19.7	16.2
OC/EC	1.91	2.79	2.03	2.26	2.20	2.10	2.40	1.90
PM ₁₀	140	48	120	44	108	41	80	39

9 ^a sd: standard deviation; OC: organic carbon; EC: element carbon.

删除的内容: components

删除的内容: of

删除的内容: 。

带格式的: 下标

带格式的: 下标

删除的内容: 。

1

2 5.3 Vertical characteristics of PM₁₀ sources

3 In order to understand the vertical characteristics of PM₁₀ sources, the chemical
4 mass balance (CMB) model was applied for source apportionment at all four sampling
5 heights. The CMB model, a useful receptor model, has been extensively used to
6 estimate source categories and contributions to the receptor based on the balance

7 between sources and the receptor (Chow et al., 2007; Watson et al., 2008). Further
8 details of CMB can be found in the relative literature. (Watson et al., 1984; Watson et
9 al., 2002; USEPA, 2004). The dataset of chemical composition in the PM₁₀ samples
10 during the measurement period and the source profiles reported in our previous
11 works(Bi, et al., 2007) were used in the CMB modeling.

12 Six source categories (coal combustion, crustal dust, cement dust, vehicle exhaust,
13 secondary sulfate and secondary nitrate) and their source contributions (μg/m³) and
14 percentage contributions (%) estimated by the CMB model are listed in Table 4. The
15 estimated source contributions (μg/m³) of all the sources showed a downward trend
16 with the increase of height. Whereas the percentage contributions (%) of secondary
17 sources (secondary sulfate and nitrate) presented a generally increasing trend with the

18 increase in height. This might be due to the fact that for the secondary sources the
19 particulate sizes are relatively smaller and the residence time of fine particle is longer.
20 Generally, secondary sources can obtain stronger influence from regional
21 contributions (Gu et al., 2011). That is to say, PM at higher heights obtain more
22 regional contributions. And, to some extent, this could reflect the characteristics at the

删除的内容:

带格式的: 非突出显示

删除的内容: Seven

删除的内容: sea salt,

删除的内容: While

删除的内容: upward

1 regional scale.

2

3

Table 4 Source contributions and percentage contributions at four different heights

		coal combustion	crustal dust	cement dust	vehicle exhaust	secondary sulfate	secondary nitrate	TOT
contribution ($\mu\text{g}/\text{m}^3$)	10m	17	16	14	20	34	23	140
	40m	16	13	10	17	33	21	120
	120m	14	12	8	15	32	24	108
	220m	12	9	4	12	25	17	80
percentage (%)	10m	12	11	10	14	24	16	88
	40m	13	11	8	14	27	18	90
	120m	13	11	8	14	29	22	97
	220m	14	11	5	15	31	21	97

4

5 **6 Vertical variation of periodicity for the time series of $\text{PM}_{2.5}$ concentrations**

6 The periodic characteristics of particulate concentration and meteorological variables

7 can reflect different scales of atmospheric processes. In this paper, the vertical

8 variation period of $\text{PM}_{2.5}$ mass concentrations were analyzed.

9 Time series of atmospheric pollutant concentration could be decomposed into

10 baseline and short-term components. Using the filtering method, short-term

11 fluctuations associated with the influence of local-scale pollution and dispersion

12 conditions can be extracted from the original measurements. After the removal of

13 local-scale effects, the time series of pollutant concentrations can be reconstructed to

14 reflect the regional scale influence.

15 **6.1 Filtering method**

16 The wavelet transform can be used to analyze time series that contain nonstationary

17 signals at many different frequencies. In this paper, we chose the Morlet wavelet

18 which is extensively used in studies of climate change and turbulence power spectrum

删除的内容: .

删除的内容: and meteorological variables

带格式的: 缩进: 首行缩进: 0 字符

删除的内容: the atmospheric boundary layer variables and particle

带格式的: 下标

删除的内容: and relative meteorological variables

删除的内容: .

带格式的: 缩进: 首行缩进: 0 字符

1 analysis (Torrence and Compo, 1998). The normalization mother wavelet is shown in

2 Eq. (4).

3
$$\psi_0(\eta) = \pi^{-1/4} e^{i\omega_0\eta} e^{-\eta^2/2} \tag{4}$$

4 where η is the nondimensional time parameter and ω_0 is the nondimensional

5 frequency. The wavelet filter time series over a set of scales can be calculated by:

6
$$x_n = \frac{\delta j \delta t^{1/2}}{C_\delta \psi_0(0)} \sum_{j=0}^J \frac{R\{W_n(s_j)\}}{s_j^{1/2}} \tag{5}$$

7 where δj is the spacing between the discrete scales, and δt is the sampling interval.

8 S_j is a set of scales related to the frequency ω . C_δ and $\psi_0(0)$ are both constants.

9
$$\omega = \frac{\omega_0 + \sqrt{2 + \omega_0^2}}{4\pi s} \tag{6}$$

10 The reconstruction then gives:

11
$$C_\delta = \frac{\delta j \delta t^{1/2}}{\psi_0(0)} \sum_{j=0}^J \frac{R\{W_\delta(s_j)\}}{s_j^{1/2}} \tag{7}$$

12 According to the conservation of total energy under the wavelet transform and the

13 equivalent of Parseval's theorem for wavelet analysis, the variance of the time series

14 is:

15
$$\sigma^2 = \frac{\delta j \delta t}{C_\delta N} \sum_{n=0}^{N-1} \sum_{j=0}^J \frac{|W_n(s_j)|^2}{s_j} \tag{8}$$

16 Both Eqs. (7) and (8) should be used to check wavelet routines for accuracy and to

17 ensure that sufficiently small values of s_0 and δj have been chosen. The values of

18 the above parameters are given in Table 5.

删除的内容: Equation ...q. (5)

域代码已更改

删除的内容: $\psi_0(\eta) = \pi^{-1/4} e^{i\omega_0\eta} e^{-\eta^2/2}$

删除的内容: η

域代码已更改

域代码已更改

删除的内容: .

域代码已更改

删除的内容: δj

域代码已更改

删除的内容: δt ...s the sampling

删除的内容:

域代码已更改

删除的内容: ω

删除的内容:

删除的内容: C_δ

删除的内容:

域代码已更改

删除的内容: $\psi_0(0)$

域代码已更改

域代码已更改

删除的内容: .

域代码已更改

删除的内容: .

删除的内容: $j1$

删除的内容: 7

带格式的

域代码已更改

删除的内容: $C_\delta = \frac{\delta j \delta t^{1/2}}{\psi_0(0)} \sum_{j=0}^J \frac{R\{W_\delta(s_j)\}}{s_j^{1/2}}$

域代码已更改

删除的内容: $\sigma^2 = \frac{\delta j \delta t}{C_\delta N} \sum_{n=0}^{N-1} \sum_{j=0}^J \frac{|W_n(s_j)|^2}{s_j}$

删除的内容: 8...) and (9...) should be

域代码已更改

删除的内容: δj

域代码已更改

带格式的

As discussed above, the wavelet transform is essentially a bandpass filter. By summing over a subset of the scales in Eq. (5), a wavelet-filtered time series can be constructed as follows:

$$x_n' = \frac{\delta j \delta t^{1/2}}{C_\delta \psi_0(0)} \sum_{j=j_1}^{j_2} \frac{R\{W_n(s_j)\}}{s_j^{1/2}} \quad (9)$$

This filter has a response function given by the sum of the wavelet functions between scale j_1 and j_2 .

Table 5. Values of the parameters of the Morlet transform in this study

C_δ	ψ_0	s_0	δt	δj	ω_0
0.776	$\pi^{-1/4}$	$2\delta t$	2	0.25	6.0

6.2 Fluctuation spectrum analysis of PM_{2.5} concentration time series at different heights

The fluctuation spectrum distribution of hourly mass concentrations of PM_{2.5} on the ground and at the height of 2, 40, 120 and 220 m were analyzed in this paper. The missing data in the time series was computed by interpolation. Because of low proportions and unconcentrated distributions in the missing data, little human interference was brought to the spectral composition of the original time series. For better comparison, normalization (standard variance 1, mean 0) of the original time series was necessary prior to power spectrum analysis.

The local and global wavelet power spectrum contours for the time series of PM_{2.5} concentrations at different heights in August are shown in Fig. 6. Contours are expressed as $\log_2(|W_n(s)|^2)$ because of large magnitudes. Area inside the thick black solid line passes the red noise standard spectral test with the 5% significance level. Area outside the blue dotted line was excluded from analysis because of poor

删除的内容: 6

删除的内容: $x_n' = \frac{\delta j \delta t^{1/2}}{C_\delta \psi_0(0)} \sum_{j=j_1}^{j_2} \frac{R\{W_n(s_j)\}}{s_j^{1/2}}$

删除的内容:

删除的内容: (10)

域代码已更改

删除的内容: j_1

删除的内容: j_2

带格式的: 字体: 倾斜

带格式的: 字体: (默认) Arial Unicode MS, (中文) Arial Unicode MS, 倾斜

带格式的: 字体: (默认) Arial Unicode MS, (中文) Arial Unicode MS

域代码已更改

域代码已更改

删除的内容: ω_0

域代码已更改

删除的内容: C_δ

删除的内容: ψ_0

域代码已更改

删除的内容: s_0

域代码已更改

删除的内容: δt

域代码已更改

删除的内容: δj

域代码已更改

域代码已更改

带格式的: 缩进: 首行缩进: 0 字符

删除的内容: m

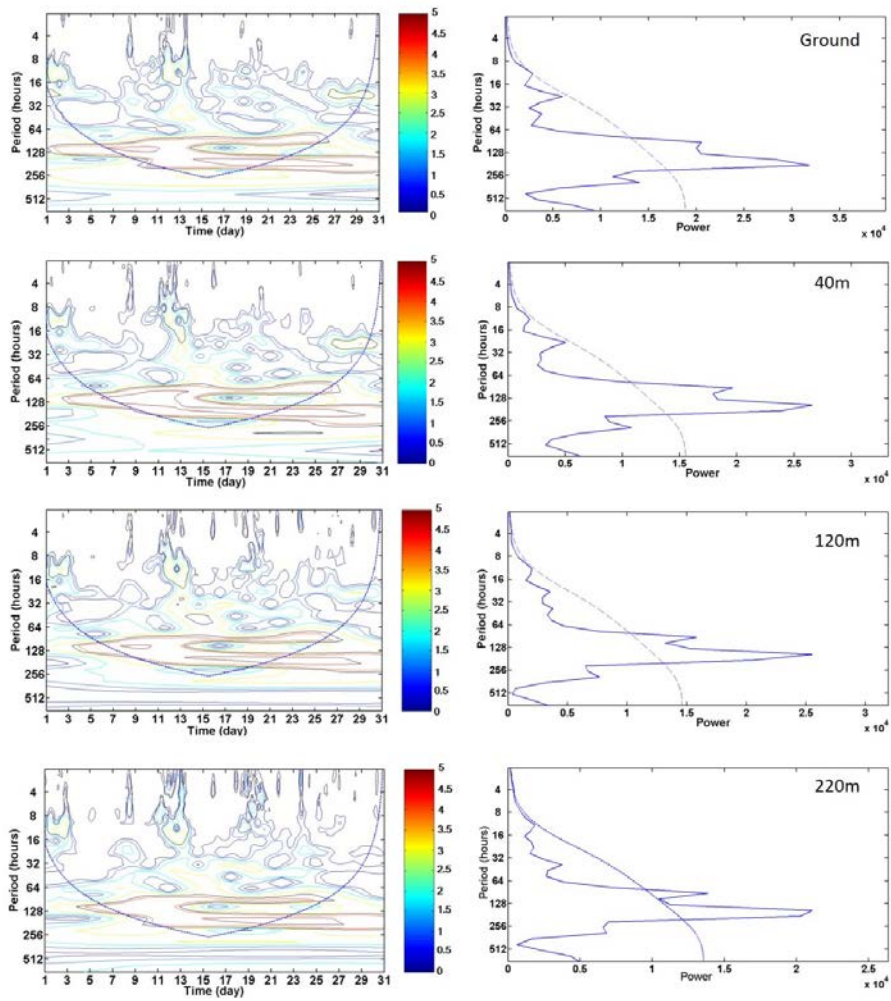
删除的内容: m

删除的内容: m

删除的内容: ure

1 reliability from the cone of influence, where edge effects become important. The
2 global wavelet spectrum $\overline{W^2}(\mathbf{s})$, which reflects characteristics of the pollutant
3 concentration time series in the frequency domain, was obtained by calculating the
4 average of local wavelet spectrums $|W_n(\mathbf{s})|^2$ over the entire sampling time domain.
5 The solid line is the global wave spectrum for the corresponding time series. The
6 dashed line is the 5% significance level, the upper area of which passes the red noise
7 standard spectral test at the 5% significance level.

8 The global wavelet power spectrum of PM_{2.5} mass concentration shows that
9 fluctuations of 6-10 days (related to weather process and regional-scale pollution) are
10 significant at each observation height, while fluctuations of 12-24 hours (mainly
11 concerned with the daily variation of atmospheric boundary layer and local pollution
12 emissions by human activities) are significant only on ground level. For the
13 fluctuations of PM_{2.5} mass concentration, wave energy of 6-10 days period reduces
14 with the increase of height. In terms of the local power spectrum, 12-24 hours period
15 can be observed in a few days on the ground. But with the increase of height, the
16 power of 12-24 hours period became weaker, only 10%-30% of that on the ground.



1
2
3
4
5
6
7
8
9
10
11

Figure 6. Local (left figure) and global (right figure) wavelet power spectrum of $PM_{2.5}$ mass concentration at different heights in August, 2009

7 Determination of regional background concentration of particulate matter

Regional PM background concentration can hardly be measured directly. Original PM concentration time series measured on the ground reflect a combination of influence from local pollution and regional-scale pollution. This study is expected to give a way to characterize the regional pollution contribution and to evaluate regional background PM concentration levels. According to the above research concerning the

带格式的: 缩进: 首行缩进: 0 字符

1 vertical distribution characteristics of particle size, chemical composition and
2 pollution sources, the atmospheric boundary layer structure, as well as the fluctuation
3 power spectrum analysis of particle mass concentration, the measurement height
4 influenced relatively less by local pollution emission was determined and impacts
5 from local-scale pollution on the short-term fluctuations have been removed from the
6 original PM concentration by wavelet transformation. The nocturnal PM_{2.5} mass
7 concentration time series with the 6-10 days period at the observation height of 220 m
8 were extracted to characterize the regional background concentration, which mainly
9 associated with the regional scale pollution within 10² km away from the
10 measurement tower.

删除的内容: the atmospheric boundary layer structure and

删除的内容: t

11 Time series of PM_{2.5} hourly concentration before and after the filtering was
12 presented in Fig. 7. Due to short-term fluctuations of pollution emission and local
13 diffusion conditions, observation errors, and etc., the original PM_{2.5} concentration time
14 series presents violent oscillation. Using wavelet transformation, the nocturnal PM_{2.5}
15 mass concentration time series with the 6-10 days period at the height of 220m was
16 extracted from the original time series. After the filtering, impacts from local-scale
17 pollution and diffusion conditions on the short-term fluctuations were considered to
18 be removed. Thus regional-scale pollution and synoptic-scale weather conditions were
19 better represented in the remaining part compared with the original PM concentration
20 time series.

带格式的: 下标

删除的内容: have

删除的内容: en

删除的内容: (shown in Figure 7)

21 The swings in the PM_{2.5} concentration data(shown in Fig. 7) were mainly resulted
22 from several meteorological processes during the measurement. According to the
23 meteorological dataset of the observation station(WMO Id.No. 54517,), precipitation
24 processes were recorded during the period of 22-24 July, with the amounts of rainfall
25 ranged from 3.2 to 94.6mm, followed by a rapid decrease in PM_{2.5} concentration on

25 July due to consequent cleaning of the air. Then, beginning on 26 July, mist paired with calm winds caused a build-up of $PM_{2.5}$ concentration until July 29. Similar meteorological processes were reported during the period of 22-25 of August, 4-9 and 20-25 of September, which resulted in the cycle of cleaning and build-up of air pollutants.

According to the method proposed in this paper, in Tianjin, the averaged regional background $PM_{2.5}$ concentrations in July, August and September, 2009 were $40 \pm 20 \mu g/m^3$, $64 \pm 17 \mu g/m^3$ and $53 \pm 11 \mu g/m^3$, respectively.

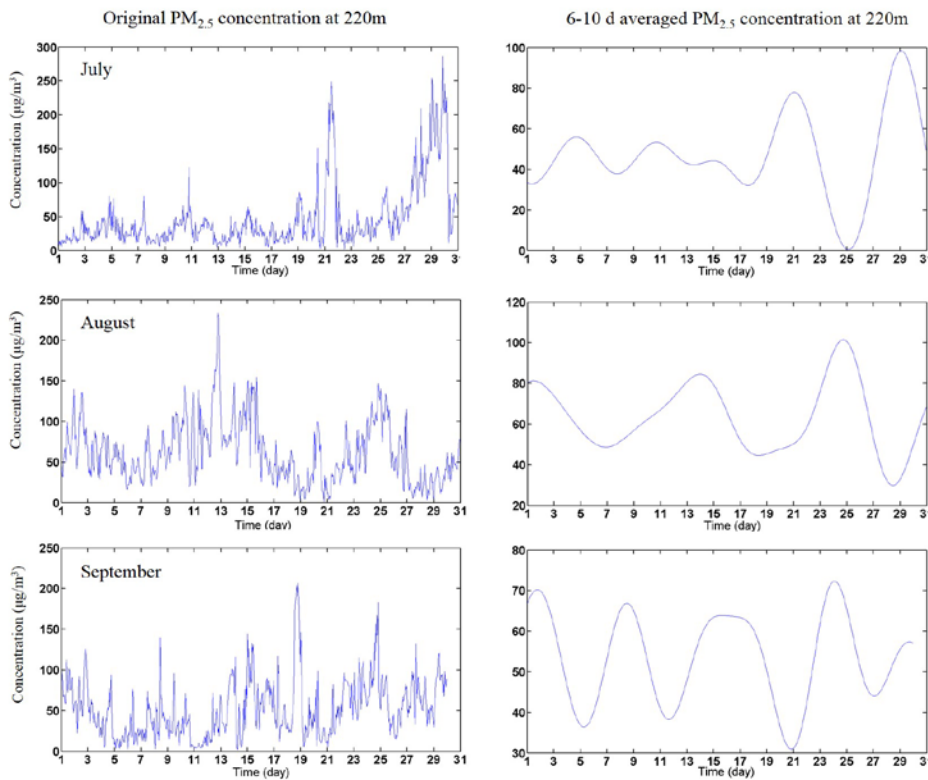


Figure 7. Time series of $PM_{2.5}$ hourly concentration before and after the filtering

8 Summary and conclusions

It is crucial for studying regional-scale PM pollution and for the development of

删除的内容: .0

删除的内容: .2

删除的内容: 3.6

删除的内容: 6.9

删除的内容: .2

删除的内容: .1

带格式的: 字体: 小四, 加粗, 字距调整二号

1 efficient joint control policy to improve understanding of the regional background
2 concentration of PM. The purpose of this study is to characterize the regional
3 pollution contribution and to evaluate regional background PM concentration levels.
4 However, regional background concentration can hardly be measured directly.
5 Original PM concentration time series measured on the ground reflect a combination
6 of influence from local pollution and regional-scale pollution. A method to estimate
7 regional background PM concentration is proposed in this paper, based on the vertical
8 variation periodic characteristics of particle mass concentration, the atmospheric
9 boundary layer structure, as well as the vertical distribution of chemical composition
10 and pollution source apportionment .

11 Based on a 255_m meteorological tower, the vertical thermodynamic and dynamic
12 characteristics of the atmospheric boundary layer in Tianjin was observed. The
13 atmospheric layer at 100-150m is considered as a transition layer, the variation
14 patterns of temperature and wind speed with height were different compared with the
15 upper and lower layers. Weak vertical gradient in the temperature profile was
16 observed over 100m. Similarly, small vertical gradient in wind speed was found over
17 150m. The turbulent intensity decreased with increase in height and the descending
18 trend is more obvious from 40 to 120_m than that of from 120 to 220m, which
19 indicates that there were fully vertical and horizontal turbulence exchanges below
20 120m of the tower, but relatively weaker exchanges over 120m. Seasonal averaged
21 nocturnal planetary boundary layer height ranges from 114 to 142 m. The observation
22 height of 220_m is just outside the NPBL, which indicates that the observation value
23 of PM concentration at 220 m at night is less affected by local primary sources near
24 the ground and is largely contributed by regional scale pollution.

25 The vertical distribution of chemical compositon in PM₁₀ filter samples also

删除的内容: Based on the spectrum analysis of vertical variation of the atmospheric boundary layer structure and particle mass concentration, as well as the vertical distribution of particle size, chemical composition and pollution source apportionment, a method to estimate regional background PM concentration is proposed in this paper. .

删除的内容: The atmospheric layer at 100-160m was considered as a special stratification

带格式的: (中文) 中文(中国)

删除的内容: the variation rules of temperature and wind speed with height were different in comparing with upper and lower layers

带格式的: (中文) 中文(中国)

删除的内容: m

删除的内容: m

删除的内容: .

删除的内容: 100m

删除的内容: 150m

删除的内容: components

带格式的: 非上标/ 下标

1 suggests that the impact of primary sources near the ground decreased with height,
2 ~~whereas~~ the impact of secondary sources mainly influenced by regional sources
3 became more prominent. The vertical distribution of percentage was different for
4 various species. Similar percentage levels were observed at the four different heights
5 for Al and Si. For the Ca and EC fractions, higher values were observed at lower
6 sampling sites. The percentages of NO_3^- , SO_4^{2-} and OC, and the OC/EC ratios were
7 obviously higher at higher sites. Source apportionment for ambient PM_{10} showed that
8 the percentage contributions of secondary sources obviously increased with height,
9 while the contribution of cement dust decreased with height. PM at higher height
10 obtained more regional contributions, and to some extent, it could reflect the
11 characteristics of the regional scale.

删除的内容: the increase in

删除的内容: while

12 The periodic characteristics of $\text{PM}_{2.5}$ mass concentration can reflect different scales
13 of atmospheric processes. In terms of global wavelet power spectrum of $\text{PM}_{2.5}$ mass
14 concentration, fluctuations of 6-10 days, related to weather processes and
15 regional-scale pollution, were significant at each observation height. While
16 fluctuations ~~with 12-24 hours period~~, mainly concerned with the daily variation of
17 atmospheric boundary layer and local pollution emissions by human activities in the
18 surface layer, were significant only on ground level. In terms of the local power
19 spectrum, 12-24 hours period can be observed in a few days on the ground. But with
20 the increase of height, the power of 12-24 hours period became weaker, only 10-30%
21 of that on the ground.

删除的内容: of

22 According to the above research, the nocturnal $\text{PM}_{2.5}$ mass concentration time
23 series with the 6-10 days period at the ~~measurement~~ height of 220m can be regarded
24 as regional background concentration, which mainly associated with the regional scale
25 pollution ~~within 10² km away from the measurement tower~~. Using wavelet

删除的内容: .

1 transformation and filtering, the nocturnal PM_{2.5} mass concentration time series with
2 the 6-10 days period at the height of 220m was extracted from the original time series.
3 After removing the impacts from local-scale pollution and diffusion conditions on the
4 short-term fluctuations, regional-scale pollution and synoptic-scale weather conditions
5 were better represented in the remaining part compared with the original PM
6 concentration time series. According to the method proposed in this paper, in Tianjin,
7 the averaged regional background PM_{2.5} concentrations in July, August and September,
8 2009 were 40 ±20 μg/m³, 64 ±17 μg/m³ and 53±11 μg/m³, respectively.

删除的内容: .

删除的内容: 40.0±20.2 μg/m³,
63.6±16.9 μg/m³ and 53.2±11.1 μg/m³

9 We attempted to put forward a new method to estimate the regional background
10 concentration of PM. Background PM concentrations are not constant but varying
11 with space and time. In future research, more analysis on the characteristics of the
12 urban boundary layer, vertical distribution of PM compositon and source
13 apportionment in different seasons and meteorological conditions will be done, and
14 background concentration ranges of PM_{2.5} for given time periods and meteorological
15 conditions will be obtained.

删除的内容: components

17 Acknowledgements

18 This work was funded by the Tianjin science and technology projects
19 (14JCYBJC22200), the Science and Technology Support Program(13ZCZDSF02100),
20 and the National Natural Science Foundation of China (NSFC) under Grant
21 No.41205089 and No.21207069. We also thank LetPub (www.letpub.com) for its
22 linguistic assistance during the preparation of this manuscript.

23

1 Reference

- 2 [Andreae, M. O., Acevedo, O. C., Araùjo, A., Artaxo, P., Barbosa, C. G. G.,](#)
3 [Barbosa, H. M. J., Brito, J., Carbone, S., Chi, X., Cintra, B. B. L., da Silva, N. F.,](#)
4 [Dias, N. L., Dias-Júnior, C. Q., Ditas, F., Ditz, R., Godoi, A. F. L., Godoi, R. H. M.,](#)
5 [Heimann, M., Hoffmann, T., Kesselmeier, J., Könemann, T., Krüger, M. L.,](#)
6 [Lavric, J. V., Manzi, A. O., Moran-Zuloaga, D., Nölscher, A. C.,](#)
7 [Santos Nogueira, D., Piedade, M. T. F., Pöhlker, C., Pöschl, U., Rizzo, L. V.,](#)
8 [Ro, C.-U., Ruckteschler, N., Sá, L. D. A., Sá, M. D. O., Sales, C. B.,](#)
9 [Santos, R. M. N. D., Saturno, J., Schöngart, J., Sörgel, M., de Souza, C. M.,](#)
10 [de Souza, R. A. F., Su, H., Targhetta, N., Tóta, J., Trebs, I., Trumbore, S.,](#)
11 [van Eijck, A., Walter, D., Wang, Z., Weber, B., Williams, J., Winderlich, J.,](#)
12 [Wittmann, F., Wolff, S., and Yáñez-Serrano, A. M.: The Amazon Tall Tower](#)
13 [Observatory \(ATTO\) in the remote Amazon Basin: overview of first results from](#)
14 [ecosystem ecology, meteorology, trace gas, and aerosol measurements, Atmos.](#)
15 [Chem. Phys. Discuss., 15, 11599–11726, doi:10.5194/acpd-15-11599-2015,](#)
16 [2015.](#)
- 17 [Bi, X., Feng, Y., Wu, J., Wang, Y., and Zhu, T.: Source apportionment of PM₁₀ in six](#)
18 [cities of northern China, Atmos. Environ., 41, 903–912, 2007.](#)
- 19 [Brown, Steven S., Thornton, Joel A., Keene, William C., Pszenny, Alexander A.](#)
20 [P., Sive, Barkley C., Dubé, William P., Wagner, Nicholas L., Young, Cora](#)
21 [J., Riedel, Theran P., Roberts, James M., VandenBoer, Trevor C., Bahreini,](#)
22 [Roya, Öztürk, Fatma, Middlebrook, Ann M., Kim, Saewung, Hübler,](#)
23 [Gerhard, Wolfe, Daniel E.: Nitrogen, Aerosol Composition, and Halogens on a](#)
24 [Tall Tower \(NACHTT\): Overview of a wintertime air chemistry field study in the](#)
25 [front range urban corridor of Colorado, J. Geophys. Res., 118, 8067–8085,](#)

1 [doi:10.1002/jgrd.50537, 2013.](https://doi.org/10.1002/jgrd.50537)

2 [Cao, J., Lee, S. C., Ho, K. F., Zhang, X. Y., Zou, S. C., Fung, K., Chow, J. C., and](#)
3 [Watson, J. G.: Characteristics of carbonaceous aerosol in Pearl River Delta Region,](#)
4 [China during 2001 winter period. Atmos. Environ., 37, 1451–1460, 2003.](#)

5 [Cao, J., Tie, X., Dabberdt, W. F., Tang, J., Zhao, Z., An, Z., Shen, Z., and Feng, Y.:](#)
6 [On the potential high acid deposition in northeastern China. J. Geophys. Res., 118,](#)
7 [4834–4846, doi: 10.1002/jgrd.50381, 2013.](#)

8 [Chameides, W. L., Yu, H., Liu, S.C., Bergin, M., Zhou, X., Mearns, L., Wang, G.,](#)
9 [Kiang, C.S., Saylor, R.D., and Luo, C.: Case study of the effects of atmospheric](#)
10 [aerosols and regional haze on agriculture: an opportunity to enhance crop yields in](#)
11 [China through emission controls. Proc. Natl. Acad. Sci., 96, 13626–13633, 1999.](#)

12 Charlson, R. J., Schwartz, S. E., Hales, J. M., Cess, R. D., Coakley, J. A., Hansen, J.
13 E., and Hofmann, D. J.: Climate forcing by anthropogenic aerosols, Science, 255,
14 423–430, 1992.

15 [Chen, J., Zhao, C. S., Ma, N., Liu, P. F., Göbel, T., Hallbauer, E., Deng, Z. Z., Ran, L.,](#)
16 [Xu, W. Y., Liang, Z., Liu, H. J., Yan, P., Zhou, X. J., and Wiedensohler, A.: A](#)
17 [parameterization of low visibilities for hazy days in the North China Plain, Atmos.](#)
18 [Chem. Phys., 12, 4935–4950, doi:10.5194/acp-12-4935-2012, 2012.](#)

19 Chow, J. C., Watson, J.G., Lowenthal, D. H., Chen, L.W. A., Zielinska, B., Mazzoleni,
20 L. R., and Magliano, K. L.: Evaluation of organic markers for chemical mass
21 balance source apportionment at the Fresno Supersite, Atmos. Chem. Phys., 7,
22 1741–1754, 2007.

23 [Chow, J. C., Watson, J. G., Chen, L. W., Rice, J., and Frank, N. H.: Quantification of](#)
24 [PM_{2.5} organic carbon sampling artifacts in US networks, Atmos. Chem. Phys., 10,](#)
25 [5223–5239, 2010.](#)

已下移 [2]: Chameides, W. L., Yu, H., Liu, S.C., Bergin, M., Zhou, X., Mearns, L., Wang, G., Kiang, C.S., Saylor, R.D., and Luo, C.: Case study of the effects of atmospheric aerosols and regional haze on agriculture: an opportunity to enhance crop yields in China through emission controls, Proc. Natl. Acad. Sci., 96, 13626–13633, 1999.

已移动(插入) [2]

已移动(插入) [3]

带格式的: 字体: Times New Roman, (中文) 中文(中国)

1 [Chow, J. C., Watson, J. G., Robles, J., Wang, X., Chen, L. W. A., Trimble, D. L.,](#)
2 [Kohl, S. D., Tropp, R. J., and Fung, K. K.: Quality assurance and quality control](#)
3 [for thermal/optical analysis of aerosol samples for organic and elemental carbon,](#)
4 [Anal. Bioanal. Chem., 401, 3141–3152, doi: 10.1007/s00216-011-5103-3, 2011.](#)

5 [Ding, G., Chen, Z., Gao, Z., Yao, W., Li, Y., Cheng, X., Meng, Z., Yu, H., Wong,](#)
6 [K., Wang, S., and Miao, Q.: The vertical structure and its dynamic characteristics](#)
7 [of PM₁₀ and PM_{2.5} in lower atmosphere in Beijing city, Sci. China, Ser. D, 35, 31–](#)
8 [44, doi: 10.1360/05yd0031, 2005.](#)

已上移 [3]: Chen, J., Zhao, C. S., Ma, N., Liu, P. F., Göbel, T., Hallbauer, E., Deng, Z. Z., Ran, L., Xu, W. Y., Liang, Z., Liu, H. J., Yan, P., Zhou, X. J., and Wiedensohler, A.: A parameterization of low visibilities for hazy days in the North China Plain, Atmos. Chem. Phys., 12, 4935–4950, doi:10.5194/acp-12-4935-2012, 2012.

带格式的: 字体: Times New Roman, (中文) 中文(中国)

9 Dockery, D.W., Pope, C. A., Xu, X., Spengler, J.D., Ware, J.H., Fay, M.E., Ferris,
10 B.G., Jr., and Speizer, F.E.: An association between air pollution and mortality in 6
11 United States cities, N. Engl. J. Med., 329, 1753–1759, 1993.

12 Dreyer, A., and Ebinghaus, R.: Poly fluorinated compounds in ambient air from ship-
13 and land-based measurements in northern Germany, Atmos. Environ., 43, 1527–
14 1535, 2009.

删除的内容: -

15 Englert, N.: Fine particles and human health-a review of epidemiological studies,
16 Toxicol. Lett., 49, 235–242, 2004.

17 [Foken, T. and Nappo, C. J.: Micrometeorology, Springer, Berlin, 308pp., 2008.](#)

18 Gu, J. X., Bai, Z. P., Li, W. F., Wu, L. P., Liu, A. X., Dong, H. Y., and Xie, Y. Y.:
19 Chemical composition of PM_{2.5} during winter in Tianjin, China, Particuology, 9,
20 215–221, 2011.

删除的内容: -

21 [Guinot, B., Roger, J. C., Cachier, H., Pucal, W., Jianhui, B., and Tong, Y. : Impact of](#)
22 [vertical atmospheric structure on Beijing aerosol distribution, Atmos. Environ., 40,](#)
23 [5167–5180, doi:10.1016/j.atmosenv.2006.03.051, 2006.](#)

24 Guo, S., Hu, M., Guo, Q., Zhang, X., Schauer, J. J., and Zhang, R.: Quantitative
25 evaluation of emission controls on primary and secondary organic aerosol sources

1 during Beijing 2008 Olympics, *Atmos. Chem. Phys.*, 13, 8303–8314, 2013.

2 Hagler, G. S. W., Bergin, M. H., Salmon, L. G., Yu, J. Z., Wan, E. C. H., Zheng, M.,
3 Zeng, L. M., Kiang, C. S., Zhang, Y. H., Lau, A. K. H. and Schauer, J. J.: Source
4 Areas and Chemical Composition of Fine Particulate Matter in the Pearl River
5 Delta Region of China, *Atmos. Environ.*, 40, 3802–3815, 2006.

6 Han, S.Q., Bian, H., Tie, X.X., Xie, Y.Y., Sun, M.L., and Liu, A.X.: Impact of
7 nocturnal planetary boundary layer on air pollutants: Measurements from a 250m
8 tower over Tianjin, China, *J. Hazard. Mater.*, 162, 264–269, 2009.

9 Han, X., Zhang, M. G., Tao, J. H., Wang, L. L., Gao, J., Wang, S. L., and Chai, F. H.:
10 Modeling aerosol impacts on atmospheric visibility in Beijing with RAMS-CMAQ,
11 *Atmos. Environ.*, 72, 177–191, 2013.

12 [Heintzenberg, J., Birmili, W., Theiss, D., and Kisilyakhov, Y.: The atmospheric](#)
13 [aerosol over Siberia, as seen from the 300 m ZOTTO tower, *Tellus B*, 60, 276–](#)
14 [285,doi: 10.1111/j.1600-0889.2007.00335.x, 2008.](#)

15 [Heintzenberg, J., Birmili, W., Seifert, P., Panov, A., Chi, X., and Andreae, M. O.:](#)
16 [Mapping the aerosol over Eurasia from the Zotino Tall Tower, *Tellus B*, 65,1–13,](#)
17 [doi: <http://dx.doi.org/10.3402/tellusb.v65i0.20062>, 2013.](#)

18 Husar, R. B., Holloway, J. M., Patterson, D. E., and Wilson, W. E.: Source areas and
19 chemical composition of fine particulate matter in the Pearl River Delta region of
20 China, *Atmos. Environ.*, 15, 1919–1928, 1981.

21 Hu, W.W., Hu, M., Yuan, B., Jimenez, J.L., Tang, Q., Peng, J.F., Hu, W., Shao, M.,
22 Wang, M., Zeng, L.M., Wu, Y.S., Gong, Z.H., Huang, X.F., and He, L.Y.: Insights
23 on organic aerosol aging and the influence of coal combustion at a regional

删除的内容: -

1 receptor site of central eastern China. *Atmos. Chem. Phys.*, 13, 10095–10112,
2 2013.

3 Hopke, P. K.: Indoor air pollution: radioactivity, *Trends Anal. Chem.*, 4, 5-6, 1985.

4 Hwang, I., Hopke, P. K., Pinto, J.P.: Source apportionment and spatial distributions of
5 coarse particles during the regional air pollution study, *Environ. Sci. Tech.*, 42,
6 3524–3530, 2008.

7 Kim, S. W., Yoon, S. C., Won, J. G., and Choi, S.C.: Ground-based remote sensing
8 measurements of aerosol and ozone in an urban area: A case study of mixing
9 height evolution and its effects on Ground-level ozone concentrations, *Atmos.*
10 *Environ.*, 41: 7069–7081, 2007.

11 Krudysz, M., Moore, K., Geller, M., Sioutas, C., and Froines, J.: Intra-community
12 spatial variability of particulate matter size distributions in Southern
13 California/Los Angeles, *Atmos. Chem. Phys.*, 9, 1061–1075, 2009.

带格式的: 字体: Times New Roman, (中文) 中文(中国)

14 Lagudu, D. R. K., Raja, S., Hopke, P. K., Chalupa, D. C., Utell, M. J., Casuccio, G.,
15 Lersch, T. L., and West, R. R.: Heterogeneity of Coarse Particles in an Urban Area,
16 *Environ. Sci. Tech.*, 45, 3188–3296, 2011.

17 Langford, A. O., Senff, C. J., Banta, R. M., Hardesty, R. M., Alvarez, R. J., Sandberg,
18 Scott P., Darby and Lisa S.: Regional and local background ozone in Houston
19 during Texas Air Quality Study , *J. Geophys. Res.*, 114, D00F12, doi:
20 10.1029/2008JD011687, 2009.

21 Lena, F. and Desiato, F.: Intercomparison of nocturnal mixing height estimate
22 methods for urban air pollution modeling, *Atmos. Environ.*, 33, 2385–2393, 1999.

23 Li, S. M.: A concerted effort to understand the ambient particulate matter in the Lower
24 Fraser Valley: the Pacific 2001 Air Quality Study, *Atmos. Environ.*, 38, 5719–5731,
25 2004.

删除的内容: -

- 1 Liu, W. X., Coveney, R. M., and Chen, J. L.: Environmental quality assessment on a
2 river system polluted by mining activities, *Appl. Geochem.*, 18, 749–764, 2003.
- 3 Liu, P. F., Zhao, C. S., Göbel, T., Hallbauer, E., Nowak, A., Ran, L., Xu, W. Y., Deng,
4 Z. Z., Ma, N., Mildenerger, K., Henning, S., Stratmann, F., and Wiedensohler, A.:
5 Hygroscopic properties of aerosol particles at high relative humidity and their
6 diurnal variations in the North China Plain, *Atmos. Chem. Phys.*, 11, 3479–3494,
7 doi:10.5194/acp-11-3479-2011, 2011.
- 8 McKendry, I. G., Stahl, K., and Moore, R. D.: Synoptic sea-level pressure patterns
9 generated by a general circulation model: comparison with types derived from
10 NCEP/NCAR re-analysis and implications for downscaling, *Int. J. Climatol.*, 26,
11 1727-1736, 2006.
- 12 Menichini, E., Iacovella, N., Monfredini, F., and Turrio-Baldassarri, T.: Atmospheric
13 pollution by PAHs, PCDD/Fs and PCBs simultaneously collected at a regional
14 background site in central Italy and at an urban site in Rome, *Chemosphere*, 69,
15 422–434, 2007.
- 16 Pal, S., Lee, T. R., Phelps, S., and De Wekker, S. F. J.: Impact of atmospheric
17 boundary layer depth variability and wind reversal on the diurnal variability of
18 aerosol concentration at a valley site, *Sci. Total Environ.*, 496, 424–434, doi:
19 <http://dx.doi.org/10.1016/j.scitotenv.2014.07.067>, 2014.
- 20 Pérez, J., Pey, S., Castillo, M., and Viana, A.: Interpretation of the variability of levels
21 of regional background aerosols in the Western Mediterranean, *Sci. Total Environ.*,
22 407, 527–540, 2008.
- 23 Ronald, C: Gaseous contaminant filtration: Keeping commercial buildings clean, *Filtr.*
24 *Separat*, 44, 24–26, 2007.

刪除的內容: -

刪除的內容: -

刪除的內容: -

1 Schmid, H. P.: Footprint modeling for vegetation atmosphere exchange studies: a
 2 review and perspective, Agric. For. Meteor., 113, 159–183, 2002.

3 Schwartz, S. E.: The white house effect—shortwave radiative forcing of climate by
 4 anthropogenic aerosols: an overview, J. Aerosol Sci., 27, 359–382, 1996.

5 Seibert, P., Beyrich, F., Gryning, S.E., Joffred, S., Rasmussene, A., and Tercierf, P.:
 6 Review and intercomparison of Operational methods for the determination of the
 7 mixing height, Atmos. Environ., 34, 1001-1027, 2000.

8 Strader, R., Lurmann, F., and Pandis, S. N.: Evaluation of secondary organic aerosol
 9 formation in winter, Atmos. Environ., 33, 4849 - 4863, 1999.

10 Shao, M., Tang, X., Zhang, Y., and Li, W.: City clusters in China: air and surface
 11 water pollution, Front. Ecol. Environ., 4, 353–361, 2006.

12 Shi, G. L., Li, X., Feng, Y. C., Wang, Y. Q., Wu, J. H., Li, J., and Zhu, T.: Combined
 13 source apportionment, using positive matrix factorization–chemical mass balance
 14 and principal component analysis /multiple linear regression–chemical mass
 15 balance models, Atmos. Environ., 43, 2929–2937, 2009.

16 Shi, G. L., Tian, Y. Z., Zhang, Y. F., Ye, W. Y., Li, X., Tie, X. X., Feng, Y. C., and Zhu,
 17 T.: Estimation of the concentrations of primary and secondary organic carbon in
 18 ambient particulate matter: Application of the CMB-Iteration method, Atmos.
 19 Environ., 45, 5692-5698, 2011.

20 Tchepel, O., Costa, A. M., Martins, H., Ferreira, J., Monteiro, A., Miranda, A.I., and
 21 Borrego, C.: Determination of background concentrations for air quality models
 22 using spectral analysis and filtering of monitoring data, Atmos. Environ., 44,
 23 106–114, 2010.

24 Tie, X. X., Brasseur, G. P., Zhao, C.S., Granierc, C., Massiea, S., Qin, Y., Wang, P.C.,

带格式的: 字体: Times New Roman, (中文) 中文(中国)

带格式的: 字体: Times New Roman, (中文) 中文(中国)

带格式的: 字体: Times New Roman, (中文) 中文(中国)

删除的内容: -

1 Wang, G., Yang, P.C., and Richter, A.: Chemical characterization of air pollution in
2 Eastern China and the Eastern United States, *Atmos. Environ.*, 40, 2607–2625,
3 2006.

4 Tie, X., Wu, D., and Brasseur, G.: Lung cancer mortality and exposure to atmospheric
5 aerosol particles in Guangzhou, China, *Atmos. Environ.*, 43, 2375–2377, 2009.

6 Tian, Y. Z., Wu, J. H., Shi, G. L., Wu, J. Y., Zhang, Y. F., Zhou, L. D., Zhang, P., and
7 Feng, Y. C.: Long-term variation of the levels, compositions and sources of
8 size-resolved particulate matter in a megacity in China, *Sci. Total Environ.*, 463,
9 462–468, 2013.

10 Torrence, C. and Compo, G. P.: A practical guide to wavelet analysis, *Bull. Amer.*
11 *Meteor. Soc.*, 79, 61–78, 1998.

12 U.S. Environmental Protection Agency (USEPA), EPA CMB8.2 User's Manual.
13 Office of Air Quality Planning and Standards, Research Triangle Park NC 27711,
14 2004.

15 Watson, J. G., Chen, L.W. A., Chow, J.C., Doraiswamy, P., and Lowenthal, D. H.:
16 Source apportionment: findings from the U.S. supersites program, *J. Air Waste*
17 *Manage. Assoc.*, 58, 265–288, 2008.

18 Watson, J.G., Cooper, J.A., and Huntzicker, J. J.: The effective variance weighting for
19 least squares calculations applied to the mass balance receptor model, *Atmos.*
20 *Environ.*, 18, 1347–1355, 1984.

21 Watson, J. G., Zhu, T., Chow, J. C., Engelbrecht, J., Fujita, E.M., and Wilson, W.E.:
22 Receptor modeling application framework for particle source apportionment,
23 *Chemosphere*, 49, 1093–1136, 2002.

24 World Health Organization (WHO), Glossary on air pollution. WHO Regional
25 Publications, Eur. Series No. 9, Regional Office for Europe, Copenhagen, 1980.

26 Wongphatarakul, V., Friedlander, S. K., and Pinto, J.P., A comparative study of PM2.5
27 ambient aerosol chemical databases, *Environ. Sci. Tech.*, 32, 3926–3934, 1998.

刪除的內容: -

刪除的內容: -

刪除的內容: -

- 1 Xiao, Z. M., Wu, J. H., Han, S. Q., Zhang, Y.F, Xu, H., Zhang, X.Y., Shi, G.L., and
2 Feng, Y.C.: Vertical characteristics and Source identification of PM10 in Tianjin, J.
3 Environ. Sci., 24, 12–115, 2012.
- 4 Zeng, Y., and Hopke, P. K.: A study of the sources of acid precipitation in Ontario,
5 Canada, Atmos. Environ., 23, 1499–1509, 1989.
- 6 [Zhu, T., Shang, J., and Zhao, D.: The roles of heterogeneous chemical processes in](#)
7 [the formation of an air pollution complex and gray haze, Sci. China, Ser. B, 54,](#)
8 [145–153, doi: 10.1007/s11426-010-4181-y, 2011.](#)